Circulation

ORIGINAL RESEARCH ARTICLE

BRD4 (Bromodomain-Containing Protein 4) Interacts with GATA4 (GATA Binding Protein 4) to Govern Mitochondrial Homeostasis in Adult Cardiomyocytes

BACKGROUND: Gene regulatory networks control tissue homeostasis and disease progression in a cell type–specific manner. Ubiquitously expressed chromatin regulators modulate these networks, yet the mechanisms governing how tissue specificity of their function is achieved are poorly understood. BRD4 (bromodomain-containing protein 4), a member of the BET (bromo- and extraterminal domain) family of ubiquitously expressed acetyl-lysine reader proteins, plays a pivotal role as a coactivator of enhancer signaling across diverse tissue types in both health and disease and has been implicated as a pharmacological target in heart failure. However, the cell-specific role of BRD4 in adult cardiomyocytes remains unknown.

METHODS: We combined conditional mouse genetics, unbiased transcriptomic and epigenomic analyses, and classic molecular biology and biochemical approaches to understand the mechanism by which BRD4 in adult cardiomyocyte homeostasis.

RESULTS: Here, we show that cardiomyocyte-specific deletion of *Brd4* in adult mice leads to acute deterioration of cardiac contractile function with mutant animals demonstrating a transcriptomic signature characterized by decreased expression of genes critical for mitochondrial energy production. Genome-wide occupancy data show that BRD4 enriches at many downregulated genes (including the master coactivators *Ppargc1a, Ppargc1b,* and their downstream targets) and preferentially colocalizes with GATA4 (GATA binding protein 4), a lineage-determining cardiac transcription factor not previously implicated in regulation of adult cardiac metabolism. BRD4 and GATA4 form an endogenous complex in cardiomyocytes and interact in a bromodomain-independent manner, revealing a new functional interaction partner for BRD4 that can direct its locus and tissue specificity.

CONCLUSIONS: These results highlight a novel role for a BRD4-GATA4 module in cooperative regulation of a cardiomyocyte-specific gene program governing bioenergetic homeostasis in the adult heart.

Arun Padmanabhan, MD, PhD*
Michael Alexanian, PhD*
Ricardo Linares-Saldana, BS*
Bárbara González-Terán, PhD
Gaia Andreoletti, PhD
Yu Huang, MD
Andrew J. Connolly, MD, PhD
Wonho Kim, PhD
Austin Hsu, BS
Qiming Duan, MD, PhD
Sarah A.B. Winchester, BA
Franco Felix, BS
Juan A. Perez-Bermejo, PhD
Qiaohong Wang, MS
Li Li, BS
Parisha P. Shah, PhD
Saptarsi M. Haldar, MD
Rajan Jain, MD†
Deepak Srivastava, MD†

*Dr Padmanabhan, Dr Alexanian, and R. Linares-Saldana contributed equally.

†Drs Jain and Srivastava contributed equally.

Key Words: epigenomics ■ mitochondria ■ myocytes, cardiac

Sources of Funding, see page 2353

https://www.ahajournals.org/journal/circ

Clinical Perspective

What Is New?

- Genetic loss of BRD4 (bromodomain-containing protein 4), an epigenetic reader protein, in adult cardiomyocytes results in cardiac dysfunction and death in mice.
- BRD4 forms a transcriptional regulatory module with GATA4, a lineage-determining transcription factor in cardiomyocytes.
- The BRD4-GATA4 module is a critical orchestrator of mitochondrial bioenergetics in the adult heart.

What Are the Clinical Implications?

- Disruptions in substrate and energy metabolism, hallmark features of human heart failure, may be driven by dysregulation of BRD4 and GATA4 function in cardiomyocytes.
- The beneficial effects of small-molecule BET (bromo- and extraterminal domain) bromodomain inhibitors in mouse models of heart failure are unlikely to be mediated exclusively by inhibition of BRD4 in cardiomyocytes, suggesting roles for other cardiac cell types and BET family members as effectors of their pharmacology.
- Identification of new BRD4 interaction partners such as GATA4 can provide new insights into developing epigenetic-based therapies for heart failure.

Heart failure (HF) is a clinical syndrome that occurs when a weakened heart is unable to maintain organ perfusion at a level adequate to meet tissue demand, resulting in shortness of breath, fatigue, and early death. This condition represents a challenge to the healthcare system, accounting for almost 2% of all medical expenditures annually and, despite the current standard of care, carries a dismal prognosis with a 5-year mortality approaching 50%.[1,2] The mainstays of therapy for HF target neurohormonal signaling pathways with β-adrenergic receptor antagonism, inhibition of the renin-angiotensin system, and augmentation of the natriuretic peptide system, all of which have improved survival in patients with HF.[3] Despite these successes, the residual burden of morbidity and mortality in HF remains high, underscoring the need for novel treatment approaches.[1]

During HF pathogenesis, hemodynamic and neurohormonal stressors activate a network of signal transduction cascades that converge on the nucleus, where specific transcription factors (TFs) drive maladaptive gene expression programs and modulate cell state.[4,5] In response, the heart undergoes pathological remodeling characterized by cardiomyocyte hypertrophy, interstitial fibrosis, and altered substrate/energy use that culminates in organ-level contractile dysfunction. Studies in animal models of HF have implicated several nodal TFs (eg, nuclear factor of activated T cells, GATA4 (GATA binding protein 4), myocyte enhancer factor 2, and nuclear factor-κB) as drivers of disease progression through their induction of gene expression programs that may provide short-term adaptation to pathological stress but whose sustained activation progressively weakens cardiac performance.[4,6] This stress-coupled activation of TFs in HF elicits global changes in chromatin structure and posttranslational modifications on histone proteins, including lysine acetylation of histone tails, TFs, and other chromatin-associated proteins. Given the central role of signal-coupled gene transcription in cardiac plasticity, manipulation of chromatin-dependent signaling as a therapeutic approach for HF is of intense interest.[7,8]

Previous work has established a crucial role for the BET (bromo- and extraterminal domain) family of acetyl-lysine reader proteins in the epigenetic control of adverse cardiac remodeling and HF pathogenesis.[9,10] There are 4 mammalian BET proteins (bromodomain-containing protein [BRD] 2, BRD3, and BRD4, which are ubiquitously expressed, and BRDT, which is testis specific) that each contain 2 tandem bromodomains that mediate acetyl-lysine binding.[11,12] BRD4 is the most studied member of this family and is a highly pursued target in cancer.[13,14] BRD4 associates with acetylated chromatin at active enhancers and promoters, where it interacts with the transcriptional machinery to coactivate transcription.[15] The ability to probe BET function in mammalian biology was accelerated by the creation of JQ1, a potent and specific small-molecule tool compound that reversibly binds the bromodomains of all BET proteins with high affinity.[16,17] JQ1 competitively and reversibly displaces BET proteins from their acetyl-lysine interaction partners on enhancers (eg, acetylated histones or acetylated TFs), thereby disrupting signaling between enhancers and promoters.[16,17] Prior studies have demonstrated that systemic delivery of JQ1 potently ameliorates HF pathogenesis in an array of rodent models.[9,10,18,19] However, the precise identities of cell types and BET isoforms that mediate these therapeutic benefits remain a major unanswered question with important translational implications. Because systemic delivery of pan-BET inhibitors such as JQ1 are unable to probe the gene-specific and cell compartment–specific functions of BRD4 in vivo, we aimed to discover the role of BRD4 in adult cardiomyocytes using a conditional genetic approach in mice.

Here, we identify a critical role for BRD4 in maintaining murine cardiac homeostasis in vivo. Because germline deletion of *Brd4* results in zygotic implantation defects and haploinsufficiency results in multisystem developmental abnormalities,[20] we generated a *Brd4* conditional allele and genetically deleted *Brd4* in adult murine cardiomyocytes. Tamoxifen-inducible genetic ablation of *Brd4* in these cells resulted in a rapid and severe reduction in global left ventricular (LV) systolic function, LV cavity dilation, and uniform death.

Integration of gene expression, genomic occupancy, and chromatin accessibility data sets demonstrated that BRD4 regulates mitochondrial gene expression. These analyses unveiled a new interaction between BRD4 and GATA4 in regulating mitochondrial gene expression and cardiomyocyte homeostasis. We confirmed a physical interaction between BRD4 and GATA4 that occurs in a bromodomain-independent fashion, with co-occupancy at thousands of promoters and enhancers across the genome in mouse cardiomyocytes. Taken together, our data reveal that BRD4 is a critical regulator of basal cardiomyocyte homeostasis and identify an unappreciated role for GATA4 in regulating metabolic gene programs in the adult heart.

METHODS

The data, analytical methods, and study materials will be made available to other researchers for purposes of reproducing the results or replicating the procedure. All relevant reagents will be maintained within the Srivastava and Jain laboratories and will be supplied on reasonable request.

RNA Sequencing, Mapping, and Quantification

For adult cardiomyocyte-enriched samples, paired-end poly(A)-enriched RNA libraries were prepared with the ovation RNA-seq Universal kit (NuGEN; strand specific). High-throughput sequencing was done with a PE75 run on a NextSeq 500 instrument (Illumina). For embryonic samples, single-end poly(A)-enriched RNA libraries were prepared with the NEBNext Ultra II DNA Library Prep kit (NEB). High-throughput sequencing was done with a SE75 run on a NextSeq 500 instrument (Illumina). Reads were mapped to the mm10 reference mouse genome using STAR (version 2.7.3a) and assigned to Ensembl genes. After read quality control, we obtained quantifications for 38293 genes in all 16 adult samples (2 day 2 Cre-control, 2 day 5 Cre-control, 3 day 2 control, 3 day 5 control, 3 day 2 *Brd4*-knockout [KO], and 3 day 5 *Brd4*-KO) and 19453 genes in all 6 embryonic samples (*Tnnt2-Cre; Brd4*$^{flox/+}$ and *Tnnt2-Cre; Brd4*$^{flox/flox}$).

Differential Gene Expression and Pathway Enrichment Analysis

To identify genes differentially expressed in Cre-control, control, and *Brd4*-KO samples, we quantified gene expression using raw counts and performed differential expression gene testing with DESeq2[21] (version 1.22.2 R package) using default settings. Statistical significance was set at a 5% false discovery rate (Benjamini-Hochberg), and significant genes were determined with an adjusted $P<0.05$ and |Log2 fold change (FC)|>1. Functional enrichment gene-set analysis for Gene Ontology (GO) terms was performed using Enrichr[22] with adjusted *P* values reported. Heat maps were generated with the Bioconductor package pheatmap (version 1.0.12) using rlog transformed counts (values shown are rlog transformed and row normalized). Volcano plots were generated with the Bioconductor package EnhancedVolcano (version 1.2.0).

Comparison of RNA-Sequencing Data Sets

To compare our RNA-sequencing (RNA-seq) results with the transcriptional changes associated with JQ1-mediated BET bromodomain inhibition, we used published expression profiles of JQ1- and vehicle-treated sham-operated mouse hearts (GSE96561). The raw counts were analyzed with DEseq2 (version 1.22.2 R package), and the correlation of the results was done by representing the Log2 FC values from each study using ggplot2 (version 3.2.0 R package). Data were taken from 3 biological replicates in each condition.

Electron Microscopy

Tissues for electron microscopic examination were fixed with 2.5% glutaraldehyde and 2.0% paraformaldehyde in 0.1 mol/L sodium cacodylate buffer (pH 7.4) overnight at 4°C. After subsequent buffer washes, the samples were postfixed in 2.0% osmium tetroxide with 1.5% $K_3Fe(CN)_6$ for 1 hour at room temperature and rinsed in distilled water. After dehydration through a graded ethanol series, the tissues were infiltrated and embedded in EMbed-812 (Electron Microscopy Sciences, Fort Washington, PA). Thin sections were stained with uranyl acetate and SATO lead and examined with a JEOL 1010 electron microscope fitted with a Hamamatsu digital camera and AMT Advantage NanoSprint500 software.

Mice

All mouse manipulations were performed in accordance with protocols approved by the Institutional Animal Care and Use Committee following guidelines described in the US National Institutes of Health's (NIH's) *Guide for the Care and Use of Laboratory Animals*.

Myh6-MCM and *Tnnt2-Cre* mice have been described previously.[23,24] *Brd4*^{flox} mice were produced by targeting C57BL/6 embryonic stem cells with a targeting vector designed to flank exon 3 (containing the canonical *Brd4* ATG) with loxP sites. The selection strategy included an FRT-flanked neomycin resistance cassette that, after excision, leaves a single FRT site within intron 2. *Brd4*^{flox} mice were genotyped with the polymerase chain reaction (PCR) primers Brd4flox_01F: 5′-GAAAGAGAAGAAGCTAACTGGC and Brd4flox_02R: 5′-GAGCAAGTATATTGGAGGGGAG that produce a 311-bp wild-type band and a 414-bp knock-in band (Figure ID in the Data Supplement). *Brd4*^{flox} mice used for embryonic studies have been described previously.[25]

Mouse Echocardiography

Echocardiography was performed blindly with the Vevo 770 High-Resolution Micro-Imaging System (VisualSonics) with a 15-MHz linear-array ultrasound transducer. The LV was assessed in both the parasternal long-axis and short-axis views at a frame rate of 120 Hz. End systole or end diastole was defined as the phase in which the LV appeared the smallest and largest, respectively, and used for ejection fraction (EF) measurements. To calculate the shortening fraction, LV end-systolic and end-diastolic diameters were measured from the LV M-mode tracing with a sweep speed of 50 mm/s at the papillary muscle. B-mode was used for 2-dimensional

measurements of end-systolic and end-diastolic dimensions. Imaging and calculations were done by an individual who was blinded to the treatment applied to each animal, and code was broken only after all data were acquired.

Histology

Isolated hearts were fixed in 2% paraformaldehyde (4 °C overnight), dehydrated through an ethanol series, embedded in paraffin, and sectioned. Antibodies used for immunohistochemistry were Brd4 (rabbit, Bethyl 00396) and cleaved caspase 3 (rabbit, Cell Signaling 9664). Hematoxylin and eosin staining was performed with standard protocols. Sections were imaged on a Nikon Eclipse 80i fluorescence microscope or Leica DMi8 inverted fluorescence microscope.

Assay for Transposase-Accessible Chromatin–Sequencing, Library Preparation, and Analysis

Cardiomyocyte samples were prepared for assay for transposase-accessible chromatin–sequencing (ATAC-seq) as previously described.[26] Aliquots of 50 000 cells were lysed with 3 mL chilled lysis buffer (3.75 mmol/L PIPES, 450 mmol/L KCl, 1% NP-40, 1% Tween-20, 1% Triton X-100 in water; pH 7.3) for 10 minutes. Nuclear pellets were transposed with 25 µL Tagment DNA Buffer, 2.5 µL Tagment DNA Enzyme (Nextera Sample Prep Kit from Illumina; FC-121-1030), and 22.5 µL nuclease-free water. Samples were incubated at 37 °C for 60 minutes. Transposed samples were purified with the QIAGEN MinElute Reaction Cleanup Kit (28204) and amplified with 25 µL NEBNext High Fidelity 2× PCR Master Mix, 1.25 mmol/L Nextera custom primers with unique barcodes, and nuclease-free water. Samples were amplified with the following PCR conditions: 72 °C for 5 minutes and 98 °C for 30 seconds and cycled at 98 °C for 10 seconds, 63 °C for 30 seconds, and 72 °C for 1 minute. Half of each sample was amplified for 12 cycles, purified, and assessed by Bioanalyzer (Agilent) for library quality. Sample concentration was quantified by Qubit (Invitrogen) before pooling. Pooled samples were sequenced with a PE75 run on a NextSeq 500 instrument (Illumina). Alignment to the mm10 reference genome was performed with Bowtie 2.2.4. Peaks were called using macs2 callpeak with the options "-p 0.1–nomodel–shift 100–extsize 200 -B–SPMR–call-summits." Peaks concordant between the 2 replicates were considered for further analysis. Motif enrichment analysis was performed with HOMER.[27]

Analysis of Publicly Available Chromatin Immunoprecipitation–Sequencing Data

Occupancy analysis for BRD4 and GATA4 was done using publicly available chromatin immunoprecipitation-sequencing (ChIP-seq) data sets (GSE52123 and GSE124008, respectively). Deeptools version 3.3.1 was used to generate the aggregation and heat map plots centered at the transcriptional start site of mm10 gene annotations (GRCm38.p6). Analysis of TF representation in our list of differentially expressed genes (DEGs) from days 2 and 5 was done with published data (GSE124008) after filtering for peaks within 1 kb of the closest annotated gene.

Immunoblotting

Adult cardiomyocytes were isolated via Langendorff perfusion of *Myh6-MCM; Brd4*$^{flox/flox}$ treated with tamoxifen (75 or 50 $\mu g \cdot g^{-1} \cdot d^{-1}$) or vehicle (corn oil) for 5 days. Whole-cell extracts were prepared by lysis in radioimmunoprecipitation assay buffer supplemented with protease and phosphatase inhibitors (Roche). Protein concentration was quantified by bicinchoninic acid assay (Thermo Fisher; 23225). Lysates were diluted in 4× lithium dodecyl sulfate sample buffer (Invitrogen), boiled at 95 °C for 5 minutes, resolved on a 3% to 8% Tris-Acetate sodium dodecyl sulphate-polyacrylamide gel electrophoresis-sodium dodecyl sulphate-polyacrylamide gel electrophoresis PAGE gel (Invitrogen), and transferred onto a polyvinylidene difluoride membrane. Membranes were blocked with 5% milk in Tris-buffered saline for 1 hour at room temperature and incubated in primary antibody at the indicated dilution overnight at 4 °C. Appropriate secondary horseradish peroxidase–conjugated antibody was added for 1 hour at a dilution of 1:5000, followed by detection with ECL Prime Western Blotting Detection Reagent (GE Life Sciences; RPN2232) and exposure to autoradiography film at various time intervals or by digital imaging (LI-COR Odyssey). Antibodies used in this study included rabbit anti-Brd4 (Abcam ab128874; 1:1000), mouse anti-vinculin (Sigma-Aldrich V9131; 1:1000), mouse anti-FLAG (Sigma F1804; 1:2000), and rabbit anti-GFP (Abcam ab290; 1:2000).

Luciferase Reporter Assay

GATA4-BRD4 transcriptional synergy reporter assay was performed with the pANF638L vector.[28] Briefly, HeLa cells were cultured in 24-well plates at 10^5 cells per well and transfected within 24 hours of seeding. Cells were cotransfected with 200 ng pANF638L vector and 20 ng pRL-TK (a Renilla luciferase control vector; Promega) in 2.4 µL FuGENE HD (Promega) and 43 µL Opti-MEM (Thermo Fisher). The transfection mix was placed in aliquots in 4 tubes (1 per condition), and the following conditions were prepared: (1) control: 600 ng empty vector; (2) GATA4: 200 ng of green fluorescent protein (GFP)-GATA4 vector plus 400 ng empty vector; (3) BRD4: 400 ng FLAG-BRD4 vector plus 200 ng empty vector; and (4) GATA4+BRD4: 200 ng GFP-GATA4 vector with 400 ng FLAG-BRD4 vector. Media was changed 24 hours after transfection, and cells were collected 48 hours after transfection. Samples were processed with the Dual Luciferase Assay System (E1960, Promega) following manufacturer's instructions and measured with a luminometer (SpectraMax i3). For analyzing the GATA4-BRD4 transcriptional activity within the *Ppargc1a* promoter, this DNA region was cloned with Cold Fusion (System Biosciences) by designing gBlocks (IDT) for the selected target region (*Ppargc1a* promoter: Mm10 chr5:51551646–51553274) with homology arms complementary to the pGL4.23 luciferase reporter vector (Promega).

Gene Knockdown Experiments on Neonatal Rat Ventricular Myocytes

Neonatal rat ventricular myocytes were isolated from hearts of 2-day-old Sprague-Dawley rat pups (Charles River) under aseptic conditions and transfected with siRNAs, as previously described.[18,29] In brief, neonatal rat ventricular myocytes were

preplated for 2 hours on tissue culture plates followed by 48 hours of exposure to BrdU in culture medium to remove contaminating nonmyocytes. Neonatal rat ventricular myocytes were plated in growth medium (DMEM, 5% FBS, 100 U/mL penicillin-streptomycin) for 48 hours. Neonatal rat ventricular myocytes were then transfected with RNAiMax (Invitrogen) and 50 nmol/L of siRNA in serum-free medium for 48 hours. Two independent siRNA probes for each target were used in tandem at a 1:1 ratio. siRNAs were purchased from Sigma Aldrich (scramble control siRNA, SIC001; Brd4 siRNAs, SASI_Rn02_00315745, SASI_Rn02_00315746; Gata4 siRNAs, SASI_Rn01_00070083, SASI_Rn01_00070084).

Coimmunoprecipitation in HEK 293T cells

HEK293T cells were plated in a 6-well plate, and 1.25 µg GFP-GATA4 and Flag-BRD4 vectors were transfected with lipofectamine 2000 (Thermo Fisher), following manufacturer's instruction. Dimethyl sulfoxide (vehicle) or JQ1 were added to cell culture media 1 day after the transfection was performed. After 48 hours, cells were lysed with 500 µL buffer A (10 mmol/L HEPES [pH 7.9], 1.5 mmol/L $MgCl_2$, 10 mmol/L KCl, 340 mmol/L sucrose, 10% glycerol, 0.1% Triton X-100 and protease inhibitors), incubated for 5 minutes at 4°C, and centrifuged at 1300*g* for 4 minutes at 4°C to pellet nuclei. Pellet was washed twice with buffer A and suspended with 500 µL of buffer B (3 mmol/L EDTA, 0.2 mmol/L EGTA and protease inhibitors). After centrifugation at 1700*g* for 5 minutes at 4°C, pellet was suspended with 400 µL lysis buffer (10 mmol/L HEPES [pH 7.9], 3 mmol/L $MgCl_2$, 5 mmol/L KCl, 140 mmol/L NaCl, 0.1 mmol/L EDTA, 0.5% NP-40, 0.5 mmol/L DTT, protease inhibitor, and 62.5 U benzonase), incubated for 45 minutes at 4°C, and centrifuged at 13200 rpm for 20 minutes at 4°C. The clear supernatant was transferred into a new tube and 30 µL lysate was saved as input. Before immunoprecipitation, 15 µL magnetic Protein G Dynabeads (Thermo Fisher) was coated with 0.5 µg M2 anti-FLAG antibody (F1804, Sigma) for 1 hour at room temperature. Lysate (300 µL) was mixed with antibody-coated Dynabeads, incubated overnight at 4°C and washed 4 times with lysis buffer. Beads were boiled for 5 minutes at 95°C in 30 µL sample buffer.

Coimmunoprecipitation in Cardiac Progenitors Cells

Human induced pluripotent stem cells were differentiated into cardiomyocytes with Wnt pathway modulation,[30] and 4×12-well plates were collected at cardiac progenitor stage (day 6 of differentiation), pooled together, and snap-frozen in liquid nitrogen. Cardiac progenitor cell pellets were lysed with 1 mL cell lysis buffer (20 mmol/L Tris-HCl pH 8, 85 mmol/L KCl, 0.5% NP-40, and protease inhibitors), incubated 10 minutes at 4°C, and centrifuged at 2500 rpm for 5 minutes at 4°C to pellet nuclei. Supernatant was removed, and pellets were resuspended in 600 µL nuclei extraction buffer (20 mmol/L HEPES pH 7.4, 0.5 mol/L NaCl, 2 mmol/L $MgCl_2$, 1 mmol/L $CaCl_2$, 0.5% NP-40, 110 mmol/L KC2H3KO2, 1 µmol/L $ZnCl_2$, benzonase, and protease/phosphatase inhibitors) and incubated for 30 minutes at 4°C. Nuclear-enriched lysates were centrifuged at maximum speed for 10 minutes at 4°C, and supernatants were transferred to a new tube and diluted with 1200 µL (1:3) immunoprecipitation dilution buffer (20 mmol/L HEPES pH 7.9, 1 mmol/L EDTA, 0.02% NP-40, and protease/phosphatase inhibitors). Before immunoprecipitation, 30 µL was saved as input. Magnetic Protein G Dynabeads (50 µL) were coated with 4 µg anti-GATA4 antibody (sc-25310X, Santa Cruz) for 1 hour at 4°C. For immunoprecipitation, 50 µL GATA4-coated beads was added to 2 mg nuclear-enriched total protein, incubated overnight at 4°C with agitation, and washed 3 times in immunoprecipitation dilution buffer. Beads were boiled for 10 minutes at 95°C in 20 µL sample buffer. Extracts and immunoprecipitates were resolved by sodium dodecyl sulphate-polyacrylamide gel electrophoresis and blotted with antibodies for the indicated targets.

Statistics and Reproducibility

Standard statistical analyses were performed with GraphPad Prism 8. When >2 conditions were to be compared, a 1-way ANOVA followed by a Tukey range test or 2-way ANOVA was used to assess the significance among pairs of conditions. When only 2 conditions were compared, a Student *t* test was used. For survival analysis, a Mantel-Cox test was used. In all the figures showing RNA-seq differential expression analysis (with DESeq2), the *P* values attained by the Wald test are corrected for multiple testing with the Benjamini and Hochberg method and thus referred to as adjusted *P* values. We used an adjusted $P<0.05$ and a |Log2 FC|>1 to determine significant genes. For all quantifications related to cardiac function and gene expression by reverse-transcription quantitative PCR, the mean±SD values are reported in the figures. For all quantifications related to cardiac function, the number of replicates is indicated as data points in the graphs. The level of significance in all graphs is represented as follow: $*P<0.05$, $**P<0.01$, $***P<0.001$, and $****P<0.0001$.

RESULTS

Loss of BRD4 in Adult Cardiomyocytes Results in Contractile Dysfunction and Lethality

We generated a *Brd4* conditional allele by engineering a homologous recombination event in mouse embryonic stem cells (Figure IA in the Data Supplement) in a pure C57BL/6 background. We designed a targeting strategy that inserted flanking loxP sites around the third exon of *Brd4*, which contains the canonical translational start site, and verified appropriate targeting in several embryonic stem cell clones by Southern blotting (Figure IB and IC in the Data Supplement). These were used to generate chimeric mice that were subsequently bred for germline transmission. Mice harboring this allele (designated *Brd-4^{flox}*) were normal, viable, and able to breed in both the heterozygous and homozygous state (Figure ID in the Data Supplement). These mice were crossed to mice harboring the Myh6-Mer-Cre-Mer (*Myh6-MCM*) allele,[23] which allows tamoxifen-inducible cardiomyocyte-specific deletion of *Brd4*. Immunofluorescence of heart tissue (Figure II in the Data Supplement) and immunoblotting of isolated

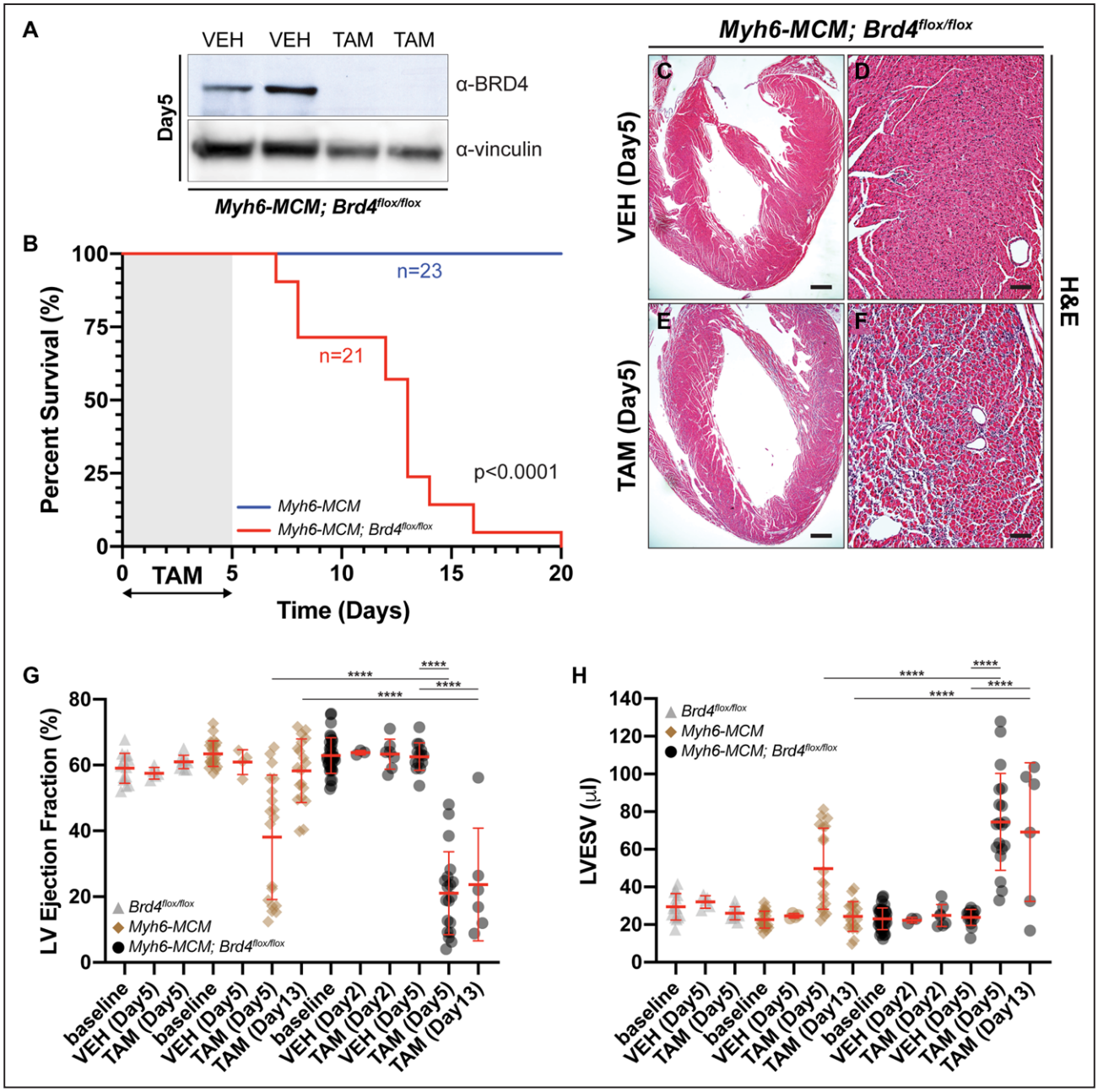

Figure 1. Adult cardiomyocyte-specific *Brd4* deletion results in acute and persistent contractile dysfunction and lethality.
A, Immunoblot of isolated *Myh6-MCM; Brd4*$^{flox/flox}$ cardiomyocyte lysates from mice treated with vehicle (VEH) or tamoxifen (TAM) for 5 days with BRD4 (bromodomain-containing protein 4) or vinculin (loading control) antibodies. **B**, Kaplan-Meier curve demonstrating survival of indicated mice treated with TAM (75 μg·g^{-1}·d^{-1}). *P* values were calculated with a Mantel-Cox test. **C** through **F**, Hematoxylin and eosin images of *Myh6-MCM; Brd4*$^{flox/flox}$ mice treated with VEH or TAM at low and high magnification. **G**, Left ventricular (LV) ejection fraction and (**H**) LV end-systolic volume (LVESV) of indicated mice treated with TAM or VEH at indicated days after injection. Individual points and mean±SD are shown. One-way ANOVA coupled with a Tukey test was used to assess significance. Scale bars = 100 μm (**D** and **F**) and 500 μm (**C** and **E**). For **B**, **G**, and **H**, ****P<0.0001 for indicated comparison.

cardiomyocyte lysates (Figure 1A) confirmed efficient loss of BRD4 protein after 5 days of tamoxifen administration.

After administration of intraperitoneal tamoxifen (75 μg·g^{-1}·d^{-1}) or vehicle (corn oil) for 5 consecutive days to adult mice, we noticed that *Myh6-MCM; Brd4*$^{flox/flox}$ animals became lethargic and ill-appearing, with several dying shortly thereafter. In a survival analysis of *Myh6-MCM; Brd4*$^{flox/flox}$ (n=21) animals treated with tamoxifen, 83% died within 14 days of the last dose of tamoxifen, with 100% mortality by 21 days. In contrast, 100% of tamoxifen-treated *Myh6-MCM* (n=23) animals survived (Figure 1B). Histological analyses revealed interstitial infiltrates in tamoxifen-treated *Myh6-MCM; Brd4*$^{flox/flox}$ animals compared with vehicle-treated controls of the same genotype (Figure 1C through 1F). We did not find any significant differences in apoptosis 5 days after tamoxifen initiation (Figure III in the Data Supplement).

We next assessed cardiac function by transthoracic echocardiography. Cohorts of *Brd4*$^{flox/flox}$ (n=14), *Myh6-MCM* (n=23), or *Myh6-MCM; Brd4*$^{flox/flox}$ mice (n=41) at 8 to 12 weeks of age were administered intraperitoneal tamoxifen (75 μg·g^{-1}·d^{-1}) or vehicle (corn oil) for 5 consecutive days. Echocardiography was performed at baseline and on days 2, 5, and 13 after tamoxifen was started. Cardiomyocyte-specific deletion of *Brd4* resulted in a significant reduction in LVEF compared with vehicle (21% versus 63%; *P*<0.0001) and LV chamber dilation (LV end-systolic volume 24 μL versus 75 μL; *P*<0.0001; Figures 1G and 1H) after 5 days of tamoxifen administration. No appreciable changes in these indices were detected after 2 days of tamoxifen treatment (EF, 63% versus 63%, *P*=NS; LV end-systolic volume, 22 μL versus 25 μL, *P*=NS). Treatment of *Brd4*$^{flox/flox}$ animals with tamoxifen or vehicle did not result in any significant changes in these parameters. Consistent with previous reports,[31] administration of tamoxifen alone for 5 days in *Myh6-MCM* animals led to a transient decrease in LV systolic function (EF, 38% versus 61%; *P*<0.0001) and LV chamber dilation immediately after tamoxifen exposure (LV end-systolic volume, 25 μL versus 50 μL; *P*<0.0001). However, the degree of LV systolic dysfunction and chamber dilation was significantly greater in *Myh6-MCM; Brd4*$^{flox/flox}$ animals compared with *Myh6-MCM* controls at the 5-day time point (EF, 21% versus 38%, *P*<0.0001; LV end-systolic volume, 75 μL versus 50 μL, *P*<0.0001). Repeat echocardiographic analysis at day 13 revealed normalization of these indices in *Myh6-MCM* controls consistent with a transient and reversible Cre-mediated toxicity. In contrast, *Myh6-MCM; Brd4*$^{flox/flox}$ animals that survived to this time point failed to demonstrate any recovery (Figure 1G and 1H). These data are consistent with our finding that only tamoxifen-treated *Myh6-MCM; Brd4*$^{flox/flox}$ mice, not equivalently treated *Myh6-MCM* mice, had a striking propensity for early mortality after tamoxifen treatment (Figure 1B). It is notable that intraperitoneal administration of tamoxifen at a lower dose (50 μg·g^{-1}·d^{-1}) for 5 consecutive days in *Myh6-MCM* (n=23) or *Myh6-MCM; Brd4*$^{flox/flox}$ (n=6) mice did not result in depletion of BRD4 protein (Figure IVA in the Data Supplement). Accordingly, noninvasive analysis demonstrated LV systolic dysfunction at day 5 that resolved by day 13 in both groups (Figure IVB and IVC in the Data Supplement). Taken together, these data demonstrate that postnatal deletion of *Brd4* in cardiomyocytes of adult mice leads to early mortality and severe systolic HF within 5 days that is sustained, suggesting an essential role for BRD4 in maintaining expression of key homeostatic gene programs in the adult cardiomyocyte.

BRD4 Regulates Mitochondrial Bioenergetic Gene Pathways

To better understand the mechanism by which BRD4, a potent transcriptional coactivator, regulates homeostasis in adult cardiomyocytes, we performed bulk RNA-seq on isolated cardiomyocytes from *Myh6-MCM; Brd4*$^{flox/flox}$ mice treated with tamoxifen (*Brd4*-KO) or vehicle (control) and *Myh6-MCM* mice treated with tamoxifen (Cre-control) (Figure VA and VB in the Data Supplement). We collected samples at 2 early time points that occurred before the onset of mortality (n≥2 biological replicates per condition): day 2 after tamoxifen (before the decrease in LVEF) and day 5 after tamoxifen (when acute HF was first detected).

Although Cre-control mice did not display mortality, we noted a transient decrease in LV systolic function after 5 days of tamoxifen treatment. Therefore, we sought to account for any gene dysregulation associated with tamoxifen-induced Cre activation in cardiomyocytes, particularly because the transcriptomic effects of this manipulation have not been reported in the literature. Using a statistical threshold to capture the vast majority of Cre-related effects on gene expression (|Log2FC|>1, adjusted *P*<0.05), we found that Cre-control cardiomyocytes demonstrated differential expression of 5038 genes compared with control cardiomyocytes at the 5-day time point (Figure VC and VD in the Data Supplement). Using these data, we defined a molecular signature after 2 and 5 days of tamoxifen treatment in *Myh6-MCM* cardiomyocytes and removed it from all subsequent analyses comparing *Brd4*-KO and control cardiomyocytes (Excel Tables I through IV in the Data Supplement).

Comparison of *Brd4*-KO and control samples at day 2 and 5 reveals a temporal increase in the number of dysregulated genes, consistent with the degree of cardiac dysfunction at each time point. We observed 101 dysregulated genes at day 2, before cardiac dysfunction (|Log2FC|>1, adjusted *P*<0.05; Figure 2A). By day 5, *Brd4*-KO cardiomyocytes demonstrated differential expression of 2094 genes compared with controls (1326 upregulated, 768 downregulated, |Log2FC|>1, adjusted *P*<0.05; Figure 2B) after removal of Cre-control dysregulated genes. GO analysis revealed a striking signature for mitochondrial bioenergetics among those genes preferentially downregulated in *Brd4*-KO cardiomyocytes, a pathway wherein BRD4 has not been implicated. GO analysis of upregulated genes in *Brd4*-KO cardiomyocytes was enriched broadly for general terms associated with cardiac stress, including fibrotic and inflammatory cellular processes, suggesting that many of these upregulated genes may be a secondary response to loss of BRD4 coactivator function in cardiomyocytes (Figure 2B).

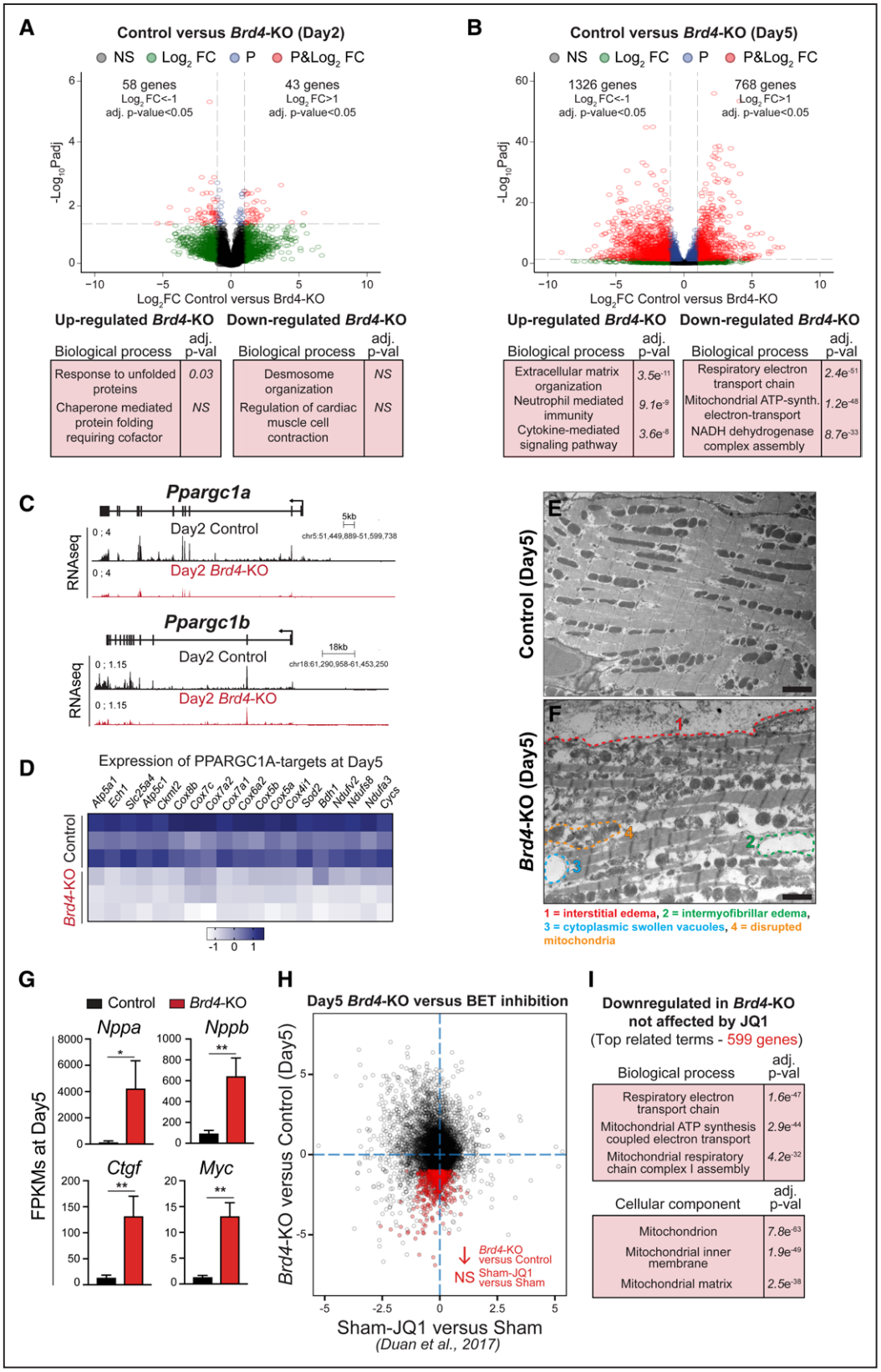

Figure 2. BRD4 regulates mitochondrial metabolic pathways in adult cardiomyocytes.
A and **B**, Volcano plots showing Log2 fold change (FC) and adjusted *P* value of individual genes 2 days (**A**) or 5 days (**B**) after *Brd4* deletion; genes differentially expressed between Cre-control and control samples have been excluded. Selected categories identified from Gene Ontology analysis from upregulated or down-regulated genes are shown below the volcano plot. Genes are assigned with specific colors after DESeq2 analysis: gray (not significant [NS]), green |Log2FC|>1, blue (adjusted *P*<0.05), or red (|Log2FC|>1 and adjusted *P*<0.05). **C**, Track view of *Ppargc1a* and *Ppargc1b* genes showing sequencing reads mapping from RNA-sequencing (RNA-seq) signature at day 2 after tamoxifen (TAM) treatment for control and *Brd4*-knockout (KO) samples. (*Continued*)

Given the marked transcriptional dysregulation of gene programs linked to mitochondrial homeostasis in *Brd4*-KO cardiomyocytes at day 5, we turned our attention to the earliest time point in our analysis (day 2) to interrogate whether established nodal regulators of mitochondrial metabolism were downregulated early after BRD4 loss. Indeed, we discovered that the expression of the transcriptional coactivators *Ppargc1a* (PPARGC1A; PGC-1α) and *Ppargc1b* (PPARGC1B; PGC-1β) was downregulated in *Brd4*-KO cardiomyocytes compared with control cardiomyocytes at this early time point, before the appearance of any LV systolic dysfunction (Figure 2C). PGC-1α and PGC-1β are known to be master regulators of mitochondrial biogenesis and oxidative phosphorylation gene programs in cardiac and skeletal muscle cells,[32,33] suggesting that the mitochondrial dysregulation may be a primary consequence of *Brd4* deletion. At day 5, expression of known targets of PPARGC1A in the heart[32] was downregulated in *Brd4*-KO cardiomyocytes compared with controls, including genes involved in oxidative phosphorylation, fatty acid oxidation, and ATP synthesis (Figure 2D). Given this signature of broad mitochondrial dysfunction identified at the transcriptional level, we performed electron microscopy to assess cardiac ultrastructure and mitochondrial morphology after BRD4 loss. Although control samples showed an organized arrangement of myofibers with normal sarcomeres (Figure 2E), *Brd4*-KO hearts demonstrated interstitial edema between cardiomyocytes (Figure 2F,1), intermyofibrillar edema within cardiomyocytes (Figure 2F,2), swollen cytoplasmic vacuoles (Figure 2F,3), and disrupted mitochondria that showed mild swelling (Figures 2F,4 and Figure VI in the Data Supplement). These findings are often observed with severe disruption of cellular metabolism, underscoring a cardiomyocyte-intrinsic gene program controlling basal mitochondrial energetics in the adult heart that is acutely sensitive to BRD4 abundance.

Pharmacological BET bromodomain inhibition with JQ1 ameliorates adverse cardiac remodeling and HF in several murine models.[9,10,18] However, JQ1 treatment does not affect exercise-induced physiological cardiac hypertrophy,[18] a form of plasticity that features upregulation of genes involved in mitochondrial biogenesis and oxidative metabolism. Transcriptional profiling of the sham-operated animals treated with JQ1 at these doses did not reveal dramatic changes, suggesting that BET bromodomain inhibition in homeostatic conditions is not associated with a pronounced gene dysregulation signature in the heart.[18] This is in stark contrast with the broad transcriptional changes that follow *Brd4* cardiomyocyte deletion that results in marked upregulation of canonical cardiac stress markers, including *Nppa*, *Nppb*, *Ctgf,* and *Myc* (Figure 2G) with concomitant downregulation of mitochondrial and metabolic genes. To assess this quantitatively, we compared gene expression changes seen with JQ1 treatment in sham-operated mice with those that follow cardiomyocyte-specific BRD4 loss in adult mice. We confirmed that global gene expression changes were poorly correlated between pharmacological BET bromodomain inhibition and BRD4 loss at day 5 after tamoxifen administration (Figure 2H). GO analysis of genes downregulated in *Brd4*-KO cardiomyocytes whose expression was unaffected by JQ1 treatment were enriched specifically for mitochondrion-related terms (Figure 2I), highlighting that transient exposure to small-molecule BET bromodomain inhibitors and *Brd4* cardiomyocyte-deletion are markedly different molecular perturbations.[7,8,34]

We next aimed to validate the importance of BRD4 in basal cardiomyocyte homeostasis using a constitutively active cardiomyocyte-specific Cre transgene with onset of expression during cardiogenesis. We crossed *Brd4^{flox}* mice with the cardiac troponin T–Cre (*Tnnt2-Cre*) allele[24] in which the rat troponin T2 cardiac promoter drives Cre recombinase expression. We identified only 1 *Tnnt2-Cre; Brd4$^{flox/flox}$* animal of 71 pups collected between postnatal days 0 and 5 (1% observed versus 17.75% expected; χ^2=34.75, P<0.001; Figure 3A). Immunofluorescence confirmed efficient cardiomyocyte loss of BRD4 in *Tnnt2-Cre; Brd4$^{flox/flox}$* mutants (Figure VII in the Data Supplement) by midgestation. Histological analysis revealed cardiac hypoplasia in *Tnnt2-Cre; Brd4$^{flox/flox}$* mutants at embryonic day 14.0 compared with littermate controls (Figure 3B–3G). Bulk RNA-seq of microdissected whole hearts from *Tnnt2-Cre; Brd4$^{flox/flox}$* mutants and *Tnnt2-Cre; Brd4$^{flox/+}$* littermate controls at embryonic day 14.0 (n=3 biological replicates per condition) revealed 260 upregulated and 405 downregulated genes (|Log2FC|>1, adjusted P<0.05; Figure 3H and Excel Table V in the Data Supplement). Consistent with our findings in adult cardiomyocytes after BRD4 loss, *Ppargc1a*, *Ppargc1b*, and known PPARGC1A-regulated genes were downregulated in *Tnnt2-Cre; Brd4$^{flox/flox}$* hearts compared with littermate controls (Figure 3I).

BRD4 Colocalizes With GATA4 at Genes Controlling Mitochondrial Bioenergy Production

Given the specific changes in gene expression caused by BRD4 deletion and the known role of BRD4 as a

Figure 2 Continued. D, Heat map of expression of PPARGC1A known targets[32] in control and *Brd4*-KO samples at day 5 after TAM treatment. **E** and **F**, Electron micrographs of *Brd4*-KO and control animals at day 5 highlighting the loss of normal mitochondrial morphology. **G**, Fragments per kilobase of transcript per million (FPKMs) of indicated genes related to cardiac stress and homeostasis in control (n=3) or *Brd4*-KO (n=3) cardiomyocytes at day 5. Error bars represent SD. **H**, Correlation analysis of difference in gene expression in day 5 *Brd4*-KO cardiomyocytes compared with sham-operated animals administered JQ1 (normalized to their respective controls). Genes highlighted in red are those that are downregulated on BRD4 loss but not significantly changed by JQ1. **I**, Gene Ontology analysis of genes that were downregulated on BRD4 loss but not affected by JQ1 treatment. Scale bars=2 μm (**E** and **F**). For **G**, *P<0.05 and **P<0.01 for indicated comparison. BRD4 indicates bromodomain-containing protein 4.

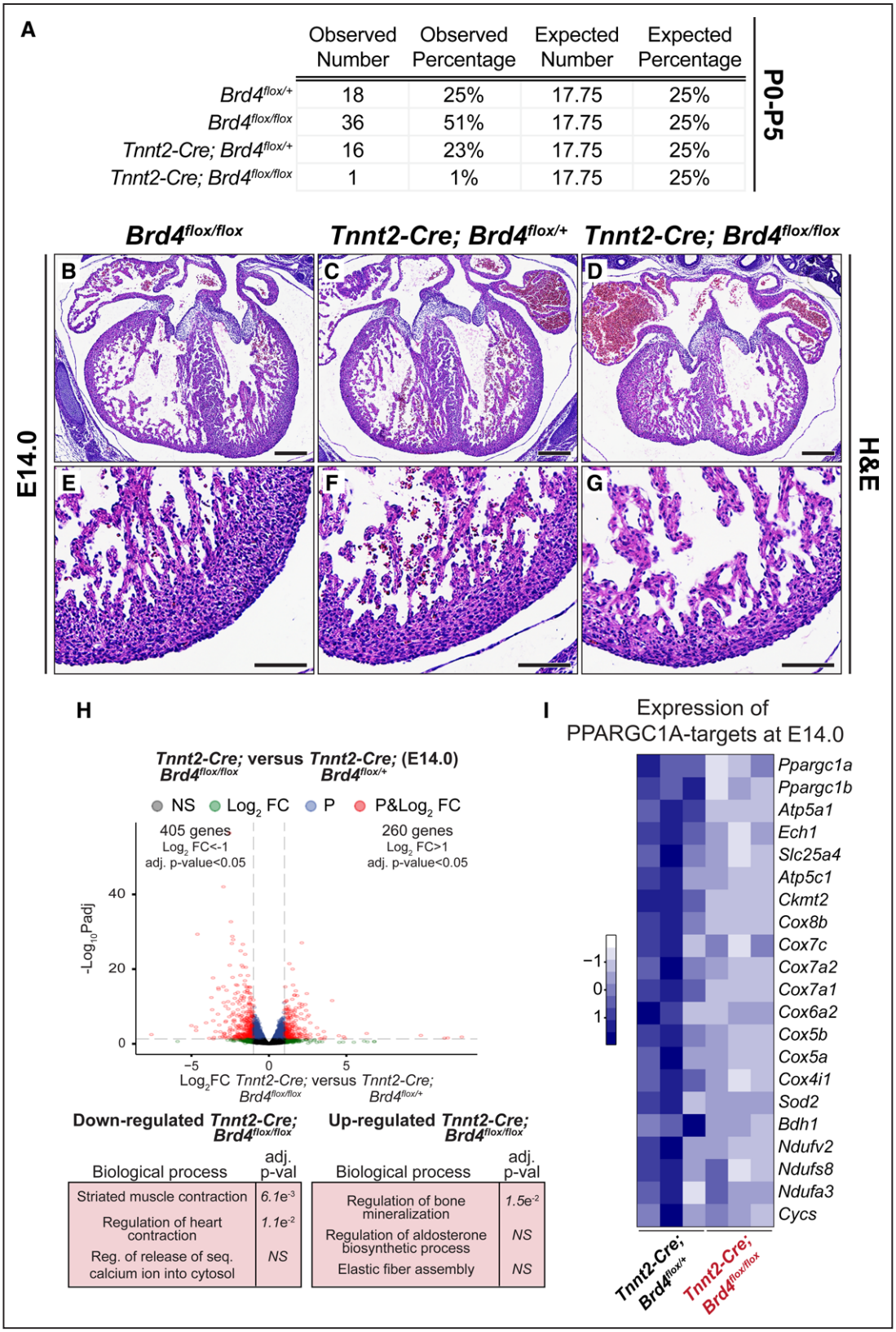

Figure 3. Constitutive cardiomyocyte-specific *Brd4* deletion is embryonic lethal and reveals BRD4 as a regulator of mitochondrial metabolic pathways in embryonic cardiomyocytes.

A, Genotyping data from parental cross of *Tnnt2-Cre; Brd4*$^{flox/+}$ and *Brd4*$^{flox/flox}$ animals demonstrating embryonic lethality in *Tnnt2-Cre; Brd4*$^{flox/flox}$ offspring at postnatal days 0 to 5 (P0–P5). **B** through **G**, Hematoxylin and eosin (H&E) images of cross sections from *Brd4*$^{flox/flox}$, *Tnnt2-Cre; Brd4*$^{flox/+}$, and *Tnnt2-Cre; Brd4*$^{flox/flox}$ embryonic hearts at embryonic day 14.0 (E14.0) at low and high magnifications. **H**, Volcano plots showing Log2 fold change (FC) and adjusted *P* value of individual genes at E14.0 between *Tnnt2-Cre; Brd4*$^{flox/+}$ and *Tnnt2-Cre; Brd4*$^{flox/flox}$ microdissected embryonic hearts. Selected categories identified (*Continued*)

coactivator of transcription, we queried changes in chromatin accessibility after cardiomyocyte-specific BRD4 loss. We performed ATAC-seq[26] on control and *Brd4*-KO cardiomyocytes isolated at day 5 (n=2 per condition). We found that 58% of ATAC-seq peaks identified in control and *Brd4*-KO samples were shared (13 428 of 23 052 total peaks; Figure 4A). In addition, we found accessible regions unique to *Brd4*-KO samples (n=5242 peaks) or control samples (n=4328 peaks), defined as regions of the genome that became accessible (gained in *Brd4*-KOs) or lost accessibility (lost in *Brd4*-KOs) upon BRD4 loss, respectively (Figure 4A). Ontology analysis of the regions that lose accessibility in *Brd4*-KO cardiomyocytes showed enrichment for regulatory elements of genes linked to cardiomyocyte identity (eg, sarcomere organization and myofibril assembly) and mitochondrial function, suggesting that BRD4 is required for those regions to be accessible (Figure 4B). Accessible regions gained in *Brd4*-KO cardiomyocytes were related to elements associated with stress responses (Figure 4B).

Because BRD4 has previously been demonstrated to interact with sequence-specific TFs in other contexts,[35–39] we hypothesized that tissue-restricted TFs may facilitate preferential enrichment of BRD4 at specific genomic loci and contribute to the sensitivity of certain gene programs to BRD4 depletion. Therefore, we performed motif analyses[27] of all the elements identified in our ATAC-seq and found enrichment for several cardiac TF motifs, including those for members of the myocyte enhancer factor 2 family, GATA4, and MEIS1 (Figure 4C). GATA4 was the only cardiac TF motif whose enrichment demonstrated a graded decrease in significance from those peaks unique to control cardiomyocytes (lost in *Brd4*-KO cardiomyocytes), shared between both conditions, and those unique to *Brd4*-KO cardiomyocytes (gained in *Brd4*-KO cardiomyocytes), suggesting that GATA4 may have preferential function in regions of active chromatin that were most sensitive to the presence of BRD4. Publicly available data sets defining the occupancy of cardiac TFs in adult heart tissue[40,41] under basal homeostatic conditions demonstrate that promoters of differentially expressed genes in *Brd4*-KO cardiomyocytes are enriched in GATA4 occupancy compared with other cardiac TFs (Figure 4D).

Given this enrichment for GATA4 occupancy in the promoters of differentially expressed genes of *Brd4*-KO cardiomyocytes, we posited that BRD4 and GATA4 may co-occupy these regions. Thus, we analyzed our previously performed BRD4 chromatin immunoprecipitation–sequencing[9] and publicly available GATA4 chromatin immunoprecipitation–sequencing data sets defining occupancy of these factors in adult mouse myocardium under basal homeostatic conditions.[40] We clustered the enrichment of BRD4 and GATA4 occupancy in regions proximal to the transcriptional start site (±1 kb) of all annotated transcripts and found that they separated into 2 clusters, one with strong occupancy of BRD4 and GATA4 (cluster 1; n=8080) and a second with little or absent co-occupancy (cluster 2; n=47 305; Figure 4E). Like our RNA-seq data, GO analysis of cluster 1 revealed genes for mitochondrial bioenergetics. Similar ontology analyses identified the mitochondrion as the most enriched cellular component, and genome-wide association studies linked single nucleotide polymorphisms from these transcripts with mitochondrial disease (Figure 4F). These data indicate that BRD4 and GATA4 co-occupy promoter regions of transcripts involved in mitochondrial energy production in adult cardiomyocytes.

Given the known role of BRD4 in enhancer-mediated transcriptional activity, we also clustered the enrichment of BRD4 and GATA4 occupancy in distal chromatin regions marked by acetylation of lysine 27 on histone H3 (H3K27Ac) in the heart[40] (Figure VIIIA in the Data Supplement). We defined 10 800 putative regulatory elements co-occupied by H3K27Ac, BRD4, and GATA4 (Figure VIIIB through VIIID in the Data Supplement) and found that 28% of the dysregulated genes after BRD4 loss were within 1 kb of a H3K27Ac/BRD4/GATA4–positive DNA element, and 49% were within 25 kb (Figure VIIIE in the Data Supplement).

Given the downregulation of *Ppargc1a* and *Ppargc1b* at day 2 after *Brd4* deletion, we specifically examined these loci for evidence of cooperative regulation by BRD4 and GATA4. Both of these genes exhibited strong enrichment for BRD4 and GATA4 at their promoters and were characterized by a putative upstream regulatory element that was also co-occupied by BRD4 and GATA4 (Figure 4G and 4H). It is notable that both of these upstream DNA elements showed decreased accessibility in *Brd4*-KO cardiomyocytes compared with controls, suggesting that accessibility of these regulatory regions is BRD4 dependent (Figure 4G and 4H). Although HF can be associated with a secondary downregulation of cardiomyocyte metabolic genes, our findings suggest a model in which a BRD4-GATA4 module controls expression of both nodal upstream transcriptional coactivators of mitochondrial metabolism and their downstream gene targets.

BRD4 Forms a Complex With GATA4 in a Bromodomain-Independent Fashion to Regulate the Transcriptional Coactivator *Ppargc1a*

Given the striking colocalization of BRD4 and GATA4 at regulatory regions controlling mitochondrial

Figure 3 Continued. from Gene Ontology analysis from upregulated or downregulated genes are shown below the volcano plot. Genes are assigned with specific colors after DESeq2 analysis: gray (not significant [NS]), green (|Log2FC|>1), blue (adjusted *P*<0.05), or red (|Log2FC|>1 or >+1 and adjusted *P*<0.05). **I**, Heat map of expression of PPARGC1A known targets[32] in *Tnnt2-Cre; Brd4*$^{flox/+}$ and *Tnnt2-Cre; Brd4*$^{flox/flox}$ in embryonic hearts at E14.0. Scale bars=250 µm (**B** through **D**) and 100 µm (**E** through **G**). BRD4 indicates bromodomain-containing protein 4.

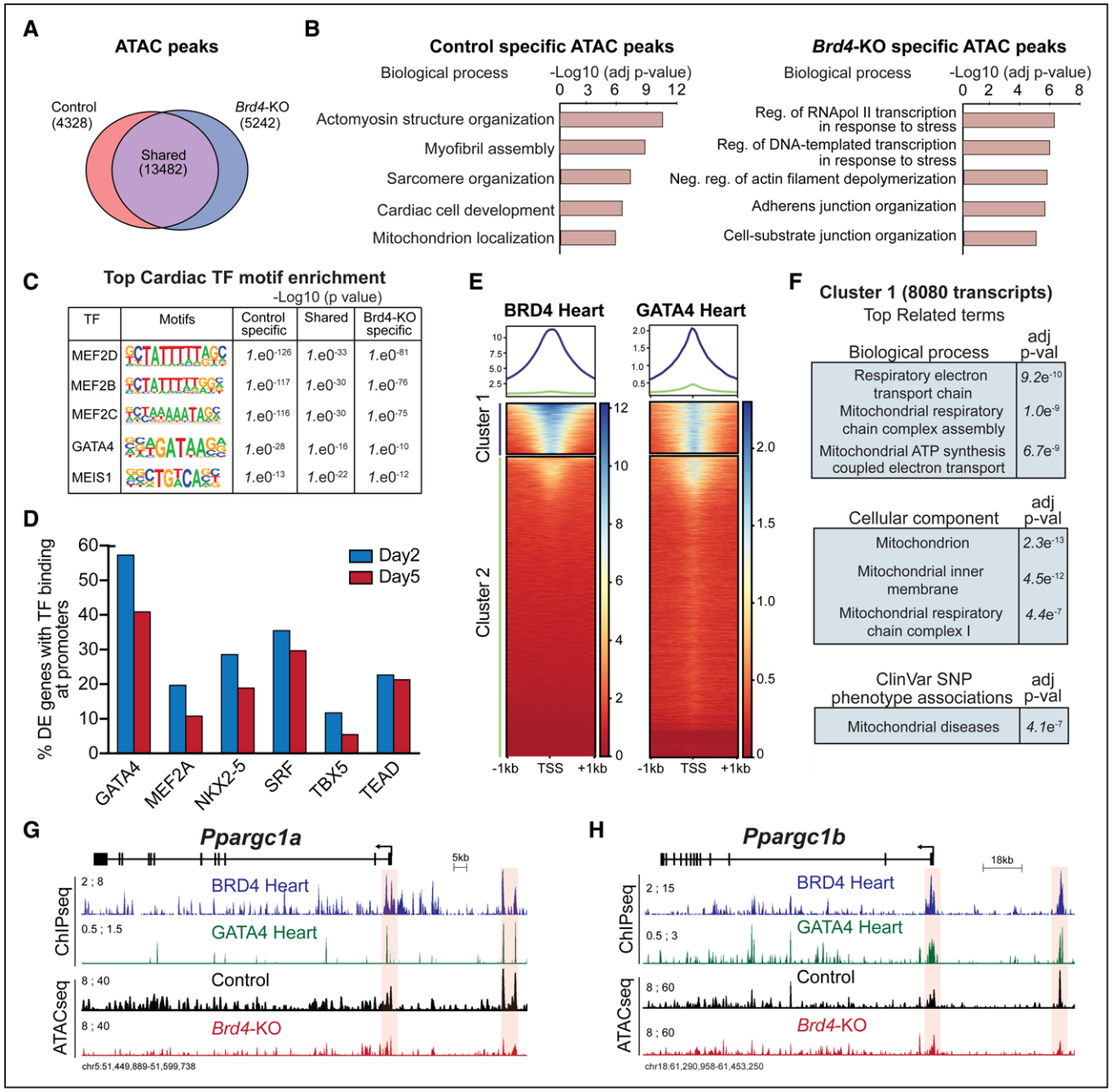

Figure 4. BRD4 and GATA4 co-occupy and regulate genes controlling mitochondrial homeostasis.
A, Venn diagram showing number of unique and shared accessible chromatin regions between control and *Brd4*-knockout (KO) samples. **B**, Top selected categories identified from Gene Ontology analysis from control and *Brd4*-KO specific assay for transposase-accessible chromatin (ATAC) regions. **C**, Motif enrichment analysis for cardiac transcription factors (TFs) in unique and shared accessible chromatin regions between control and *Brd4*-KO samples. **D**, Number of differentially expressed genes between control and *Brd4*-KO at days 2 and 5 occupied by cardiac TFs[40,41] at their promoters (±1 kb transcriptional start site [TSS]). **E**, Heat maps showing enrichment of BRD4 and GATA4 chromatin immunoprecipitation (ChIP) signals from adult mouse hearts under basal homeostatic conditions at gene promoters (±1 kb TSS, 55 386 mm10 annotated transcripts) ordered by BRD4 intensity identifies a cluster of strongly bound transcripts (cluster 1, n=8080). **F**, Gene Ontology analysis of cluster 1 genes identified enriched terms for biological processes, cellular components, and single-nucleotide polymorphism–phenotype (SNP) associations. **G** and **H**, Track view of *Ppargc1a* and *Ppargc1b* genes showing sequencing reads mapping from BRD4 and GATA4 ChIP-sequencing (ChIP-seq) as well as control and *Brd4*-KO ATAC-sequencing (ATAC-seq) at day 5 after tamoxifen treatment. The promoter region and a putative regulatory element for each gene are highlighted in red. BRD4 indicates bromodomain-containing protein 4.

bioenergetics, we hypothesized that BRD4 and GATA4 may functionally coregulate these genes. We first tested the ability of BRD4 and GATA4 to transactivate the *Nppa* promoter-luciferase reporter, a well-established gene reporter construct and known GATA4 target,[42,43] in transient transfection assays. Transfection of BRD4 or GATA4 alone resulted in activation of this reporter, whereas cotransfection of both together led to additive transcriptional activation (Figure 5A). We then performed the same assay for the promoter element of

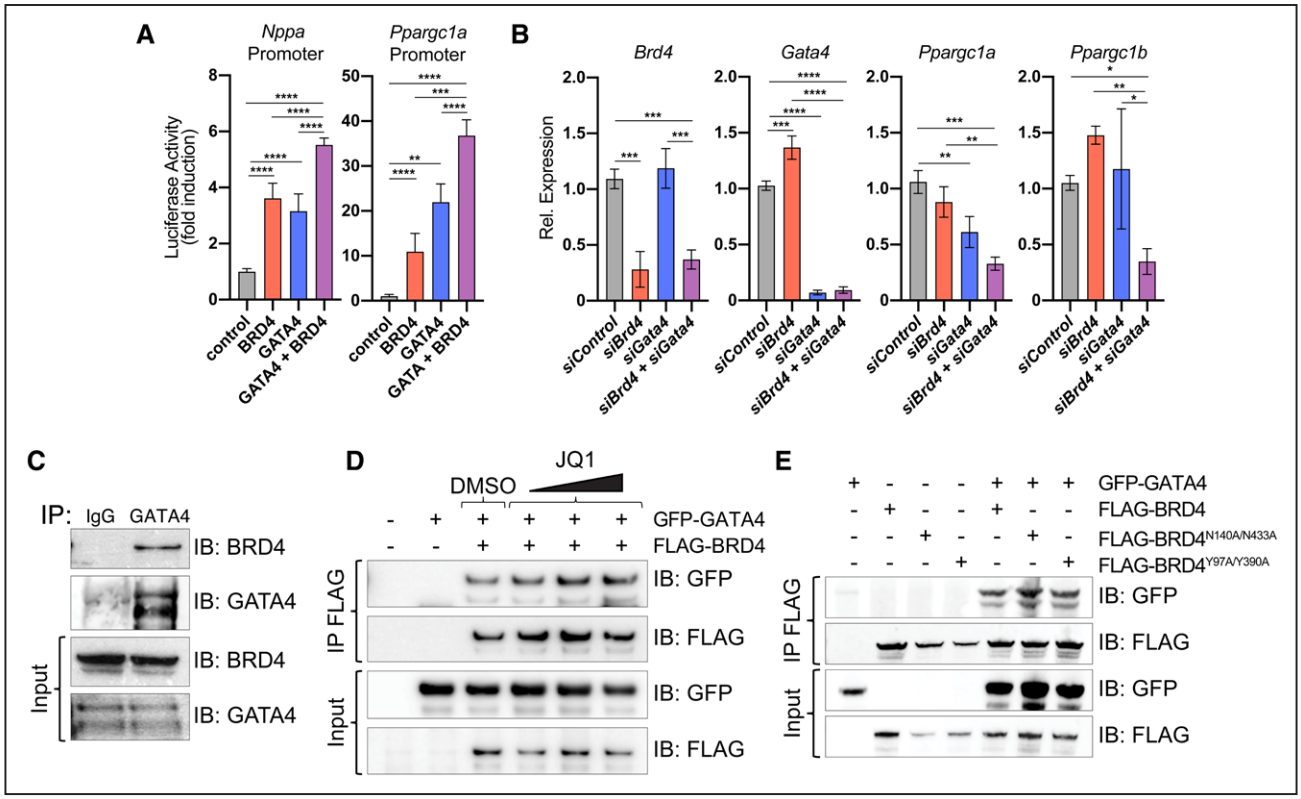

Figure 5. BRD4 and GATA4 interact in a bromodomain-independent manner to control the master regulator of mitochondrial homeostasis *Ppargc1a*. **A**, Gene reporter assay showing activation of indicated luciferase reporters on addition of plasmids encoding indicated proteins. Statistical significance is shown between control and GATA4+BRD4 vs all other individual conditions (n=4). **B**, Relative expression by reverse-transcription quantitative polymerase chain reaction in neonatal rat ventricular myocytes. Statistical significance is indicated between *siControl* and *siGata4* + *siBrd4* vs all other individual conditions (n=3). One-way ANOVA coupled with a Tukey test was used to assess significance. **C**, Immunoprecipitation (IP) of endogenous protein from human cardiac progenitor cells using anti-GATA4 or anti-IgG antibody and immunoblotting (IB) with anti-BRD4 or anti-GATA4 antibody demonstrate that endogenous BRD4 coimmunoprecipitates with GATA4 but not immunoglobulin G (IgG). **D**, IP of FLAG-BRD4–overexpressed in HEK293 cells followed by IB with anti–green fluorescent protein (GFP) or anti-FLAG antibodies demonstrates that GFP-GATA4 still co-IPs with BRD4 even in the presence of increasing doses of JQ1 or dimethyl sulfoxide (DMSO) as control. **E**, IP of FLAG-BRD4, FLAG-BRD4$^{N140A/N433A}$, and FLAG-BRD4$^{Y97A/Y390A}$ in HEK293 cells followed by IB with anti-GFP or anti-FLAG antibodies indicates co-IP of BRD4 mutants with GFP-GATA4. For **A** and **B**, **P*<0.05, ***P*<0.01, ****P*<0.001, and *****P*<0.0001 for indicated comparisons. BRD4 indicates bromodomain-containing protein 4.

Ppargc1a that showed strong co-occupancy of BRD4 and GATA4 (Figure 4G). A luciferase reporter construct containing the *Ppargc1a* promoter also demonstrated additive coregulation by BRD4 and GATA4 (11-fold activation with BRD4, 22-fold activation with GATA4, and 37-fold activation with GATA4+BRD4; Figure 5A). Conversely, in neonatal rat ventricular myocytes, we observed a greater downregulation of *Ppargc1a* and *Ppargc1b* expression on siRNA-mediated knockdown of both *Brd4* and *Gata4* compared with either factor individually (Figure 5B). We do note that individual *Brd4* knockdown did not phenocopy the decrease in *Ppargc1a*/*Ppargc1b* expression seen in vivo, which may reflect differences attributable to this immature cellular system or the partial knockdown of *Brd4*. Taken together, these data suggest a functional cooperativity between BRD4 and GATA4.

Immunoprecipitation of endogenous GATA4 protein from human induced pluripotent stem cell–derived cardiac progenitor cell lysates (which express high levels of GATA4) followed by immunoblotting for BRD4 demonstrated that endogenous human GATA4 and BRD4 interact in cardiomyocyte progenitors (Figure 5C). When cotransfected in 293T cells, GFP-tagged GATA4 and FLAG-tagged BRD4 also coimmunoprecipitated (Figure 5D). GATA4 contains 4 lysine residues that are targets of p300-mediated acetylation.[44] These residues are conserved in GATA1, which has previously been demonstrated to bind to BRD3 in an acetyl-lysine–dependent fashion via the bromodomains of BRD3.[45,46] However, increasing concentrations of JQ1 had no appreciable effect on the ability of BRD4 and GATA4 to interact in 293T cells (Figure 5D). The tertiary structure of the BRD4 bromodomain bound to acetyl-lysine[11] and JQ1[17] has been extensively characterized, revealing 2 amino acids in each bromodomain that are critical for mediating interactions with acetylated-lysine targets (N140 and Y97 of bromodomain 1; N433 and Y390 of bromodomain 2).[47–50] BRD4 mutant constructs harboring N140A and N433A mutations or Y97A and Y390A retained the ability to interact with GATA4 (Figure 5E), consistent with this interaction occurring independently

of the acetyl-lysine recognition activity of BRD4. This observation is also consistent with the disparity in cardiac phenotype of cardiomyocyte-specific *Brd4* deletion and JQ1 treatment in mice.

DISCUSSION

In this report, we leveraged a newly developed mouse line harboring a conditional *Brd4* allele and unbiased transcriptomic and epigenomic assays to dissect the role of this transcriptional coactivator in adult cardiomyocyte homeostasis in vivo. Acute depletion of BRD4 in adult cardiomyocytes caused rapid onset of systolic HF within 5 days, leading to 100% lethality by 20 days. Transcriptomic profiling of cardiomyocytes from *Brd4*-KO mice at day 5 revealed robust and relatively specific downregulation of gene programs important for mitochondrial energetics and homeostasis. Integrated analysis of BRD4-dependent gene expression and chromatin accessibility in adult cardiomyocytes identified that GATA4 binding sites were preferentially enriched in the regulatory regions of BRD4-dependent genes. Our results reveal that BRD4 and GATA4 colocalize across the genome at loci relevant to mitochondrial bioenergy production and identify a novel bromodomain-independent protein complex formation between BRD4 and this key cardiac TF. These findings highlight an unexpected role for both BRD4 and GATA4 in controlling a metabolic gene expression program in cardiomyocytes, including direct regulation of *Ppargc1a* and *Ppargc1b*. Although the interaction with GATA4 is important, our data do not preclude the possibility of BRD4 to complex with other cardiac TFs in activating cardiac gene expression programs. Important aspects of the BRD4 cardiomyocyte-deletion phenotype are likely mediated through interactions with GATA4 and other transcriptional regulators. Future work aimed at defining the specific regions of BRD4 and GATA4 that mediate their interaction and the consequences of selectively abrogating BRD4-GATA4 complex formation will be important.

BET proteins have emerged as pharmacological targets in cancer and chronic diseases, including HF.[7,8,14,51–53] In animal models of HF, JQ1 administration improves cardiac function, decreases fibrosis, and attenuates activation of inflammatory and profibrotic gene programs.[9,10,18] Clinical-grade BET bromodomain inhibitors are in trials for the treatment of a variety of malignancies[14] and, although chemically diverse, share a common structural motif that reversibly binds the BDs of all BET family members and transiently displaces them from their endogenous binding partners. BRD2, BRD3, and BRD4 are ubiquitously expressed, and the relevant tissue compartments in which they function in vivo remain unknown. Small-molecule proteolysis targeting chimeras that degrade BET proteins represent a closer equivalent to genetic deletion,[54–56] but these again are neither cell nor BET isoform specific. Therefore, these pharmacological approaches offer limited insight into the cell-type and isoform specificities associated with beneficial responses of these compounds in disease models. Our data show that acute BRD4 depletion in cardiomyocytes leads to rapid-onset systolic HF and mortality, highlighting a sharp contrast with the beneficial effects of small-molecule BET bromodomain inhibitors in treating adult mice with HF. These data are consistent with earlier studies and suggest that the dominant cellular targets of JQ1 in the context of HF are noncardiomyocytes such as fibroblasts and immune cells.[18,57] Further dissection of these cell compartment- and gene-specific effects in the context of HF using conditional mice for each BET allele will be a fruitful area of study. Although small-molecule BET bromodomain inhibitors and conditional gene deletion approaches manipulate BET proteins by very different mechanisms, our findings underscore the importance of understanding the specific cell types that mediate the beneficial effects and potential liabilities of BET bromodomain inhibitor therapy.

Our studies also suggest a previously unrecognized role for GATA4, one of the most studied TFs in cardiac biology, in cardiomyocyte metabolism and mitochondrial homeostasis. GATA4 is a well-established lineage determining TF for cardiomyocytes whose role in cardiac development and human congenital heart disease has been studied extensively.[58,59] Because ectopic *Gata4* expression (along with *Mef2c* and *Tbx5*) can induce conversion of cardiac fibroblasts into induced cardiomyocytes,[60–62] much effort has focused on dissecting the molecular mechanisms by which GATA4 regulates cellular identity.[63,64] In the adult heart, GATA4 plays an important role in stress responsiveness and regulation of proangiogenic genes.[65,66] Our data indicate that BRD4 also governs mitochondrial homeostasis in the adult heart and suggest that the preference of BRD4 to occupy certain loci may be mediated, in part, through an interaction with GATA4. They further demonstrate that a BRD4-GATA4 coregulatory module orchestrates mitochondrial gene expression programs by regulating both nodal upstream regulators of these transcriptional programs (PGC-1α and PGC-1β) and their downstream targets, suggesting transcriptional control via a tiered, feed-forward circuitry.

Cardiac contractile function is highly dependent on the ability of working cardiomyocytes to sustain very high rates of mitochondrial oxidative phosphorylation and efficiently transfer energy.[67,68] Cardiomyopathies caused by loss-of-function variants in key mitochondrial genes underscore the direct link between mitochondrial dysfunction and contractile failure.[69,70] Consistent with these findings, deletion of key transcriptional regulators of mitochondrial homeostasis in murine cardiomyocytes, including PPARGC1A and ERRα, causes cardiomyopathy

and HF.[32,33,71] Electron microscopy of *Brd4*-KO hearts revealed myofiber degeneration and sarcomere disarray. This phenotype may be a downstream consequence of mitochondrial dysfunction, which can lead to pleiotropic defects in cellular homeostatic processes (eg, protein quality control and calcium handling). In parallel, BRD4 may also play a primary role in coactivating key genes that are critical for sarcomere assembly and maintenance. GATA4 is required for cardiac morphogenesis and directly activates sarcomere genes during cardiac lineage commitment,[72] raising the possibility that the BRD4-GATA4 axis in adult cardiomyocytes may regulate sarcomere genes in addition to mitochondrial programs. Given our finding that BRD4 is required for normal cardiogenesis and the previous discovery of GATA4 haploinsufficiency in congenital heart disease,[58] it will be interesting to determine whether BRD4-GATA4 regulation is also critical for normal cardiac development. Dissecting the mechanisms by which BRD4 deficiency leads to both mitochondrial dysfunction and sarcomere disarray in cardiomyocytes will be an important area of future investigation.

Our experiments have also revealed critical new knowledge about a commonly used reagent, the *Myh6-MCM* transgenic mouse.[23] This mouse strain has become a standard tool for inducible cardiomyocyte-targeted deletion of conditional alleles. This transgene expresses a Cre recombinase flanked by mutated estrogen receptor ligand-binding domains insensitive to endogenous estrogen (but responsive to exogenously administered tamoxifen) under the control of a α-myosin heavy chain (*Myh6*) promoter. Prior reports have demonstrated a transient myopathy associated with Cre nuclear translocation after tamoxifen administration in these animals and warned of potential confounding in assessment of acute phenotypes that result from ablation of any gene of interest.[31] We define the first transcriptomic characterization of this transient myopathy (Figure V in the Data Supplement) at days 2 and 5 after tamoxifen administration. Hence, accounting for gene expression changes on induction of this transgene will be critical in the interpretation of results generated using these mice, providing a major resource for the field.

Apart from potential clinical application of BET bromodomain inhibitors for therapeutic purposes, compounds like JQ1 have emerged as powerful tools for investigating enhancer biology.[73] Indeed, much of the field focuses on the bromodomain-mediated functions of these proteins. In addition to acetylated histones, BET proteins bind acetylated TFs and modulate their transcriptional output. A bromodomain-dependent interaction between BRD3 and GATA1 is important for erythroid maturation.[45] Likewise, bromodomain-dependent interactions between BRD4 and p65/RelA-K310ac have been implicated in innate immunity,[35] and similar interactions with hematopoietic TFs (including PU.1, FLI1, and ERG) are essential for acute myeloid leukemia pathogenesis.[39] The advent of small molecules with a selectivity for bromodomain 1 versus bromodomain 2 has stimulated further interest in dissecting the relative contribution of each of these domains in a variety of cellular contexts.[74,75] However, the BETs are large proteins that can scaffold complexes through multiple domains outside of their BDs. The BRD4 C-terminal domain interacts with the PTEFb complex,[76,77] and the BRD4 extraterminal domain interacts with the histone methyltransferase NSD3.[78,79] Unbiased interaction screens for BET family members have been performed in the presence and absence of JQ1, demonstrating a number of bromodomain-independent interacting partners for each of the ubiquitously expressed BET family members.[80] Our data identify a novel, bromodomain-independent interaction between BRD4 and GATA4, suggesting a mechanism by which a broadly expressed chromatin coactivator can be preferentially targeted to specific genomic loci by associating with a tissue-enriched DNA-binding TF. JQ1-mediated inhibition in vivo would not be expected to disrupt the BRD4-GATA4 interaction, consistent with the differences seen between the therapeutic effects of JQ1 and the deleterious consequences of *Brd4* deletion in vivo. Our work highlights a critical need to better understand structure-function relationships of BRD4 outside of the BDs, findings that will provide general insight into the molecular underpinnings of cell-specific gene regulation and inform novel therapeutic approaches for HF and other cardiovascular diseases.

CONCLUSIONS

In this study, we discover a BRD4-GATA4 protein module that regulates mitochondrial gene expression and bioenergetic homeostasis in adult cardiomyocytes.

ARTICLE INFORMATION

Received April 16, 2020; accepted October 5, 2020.

This manuscript was sent to Prof Jun Chen, Guest Editor, for review by expert referees, editorial decision, and final disposition.

The Data Supplement is available with this article at https://www.ahajournals.org/doi/suppl/10.1161/circulationaha.120.047753.

Correspondence

Deepak Srivastava, MD, Gladstone Institute of Cardiovascular Disease, 1650 Owens Street, San Francisco, CA 94158; or Rajan Jain, MD, Perelman School of Medicine, 3400 Civic Center Boulevard, Philadelphia, PA 19104. Email deepak.srivastava@gladstone.ucsf.edu or jainr@pennmedicine.upenn.edu

Affiliations

Gladstone Institute of Cardiovascular Disease, San Francisco, CA (A.P., M.A., B.G.-T., Y.H., A.H., Q.D., S.A.B.W., F.F., J.A.P.-B., S.M.H., D.S.). Division of Cardiology, Department of Medicine (A.P., S.M.H.), Bakar Computational Health Sciences Institute (G.A.), Department of Pathology (A.J.C.), Department of Pediatrics (D.S.), and Department of Biochemistry and Biophysics (D.S.), University of California, San Francisco. Institute of Regenerative Medicine, Penn Cardiovascular Institute, Departments of Medicine and Cell and Developmental Biology, Perelman School of Medicine, Philadelphia, PA (R.L.-S., W.K., Q.W.,

L.L., P.P.S., R.J.). Roddenberry Center for Stem Cell Biology and Medicine at Gladstone, San Francisco, CA (D.S.). Dr Haldar is currently at Amgen Research, Cardiometabolic Disorders, South San Francisco, CA.

Acknowledgments

The authors thank the Srivastava and Jain laboratories for critical discussions and feedback; the Penn Electron Microscopy Core for assistance with sample preparation and imaging for electron microscopy; and the Gladstone Genomics Core for library preparation and sequencing for transcriptional analyses. They thank Keiko Ozato for experimental reagents. They also thank Reuben Thomas from the Gladstone Bioinformatics Core for assistance with statistical analyses.

Sources of Funding

Dr Padmanabhan is supported by the Tobacco-Related Disease Research Program (grant 578649), A.P. Giannini Foundation (grant P0527061), Michael Antonov Charitable Foundation Inc, and the Sarnoff Cardiovascular Research Foundation. Dr Alexanian is supported by the Swiss National Science Foundation (grant P400PM_186704). R. Linares-Saldana is supported by National Institutes of Health grant F31 HL147416. Dr Haldar was supported by National Institutes of Health grant R01 HL127240. Dr Jain is supported by the Burroughs Wellcome Career Award for Medical Scientists, Gilead Research Scholars Award, American Heart Association, Allen Foundation, National Science Foundation CMMI-1548571, and National Institutes of Health grant R01 HL139783. Dr Srivastava is supported by National Institutes of Health grants P01 HL098707, P01 HL146366, R01 HL057181, and R01 HL127240; the Roddenberry Foundation; the L.K. Whittier Foundation; and the Younger Family Fund. This work was also supported by the National Institutes of Health/National Center for Research Resources grant C06 RR018928 to the Gladstone Institutes.

Disclosures

Dr Srivastava is scientific cofounder, shareholder, and director of Tenaya Therapeutics. Dr Haldar is an executive, officer, and shareholder of Amgen, Inc and is a scientific cofounder and shareholder of Tenaya Therapeutics.

Supplemental Material

Data Supplement Figures I–VIII
Data Supplement Excel Tables I–V

REFERENCES

1. Virani SS, Alonso A, Benjamin EJ, Bittencourt MS, Callaway CW, Carson AP, Chamberlain AM, Chang AR, Cheng S, Delling FN, et al; American Heart Association Council on Epidemiology and Prevention Statistics Committee and Stroke Statistics Subcommittee. Heart disease and stroke statistics–2020 update: a report from the American Heart Association. *Circulation.* 2020;141:e139–e596. doi: 10.1161/CIR.0000000000000757
2. Timmis A, Townsend N, Gale CP, Torbica A, Lettino M, Petersen SE, Mossialos EA, Maggioni AP, Kazakiewicz D, May HT, et al; European Society of Cardiology. European Society of Cardiology: cardiovascular disease statistics 2019. *Eur Heart J.* 2020;41:12–85. doi: 10.1093/eurheartj/ehz859
3. Burnett H, Earley A, Voors AA, Senni M, McMurray JJV, Deschaseaux C, Cope S. Thirty years of evidence on the efficacy of drug treatments for chronic heart failure with reduced ejection fraction: a network meta-analysis. *Circ Heart Fail.* 2017;10:e003529.
4. van Berlo JH, Maillet M, Molkentin JD. Signaling effectors underlying pathologic growth and remodeling of the heart. *J Clin Invest.* 2013;123:37–45. doi: 10.1172/JCI62839
5. Hill JA, Olson EN. Cardiac plasticity. *N Engl J Med.* 2008;358:1370–1380. doi: 10.1056/NEJMra072139
6. Akazawa H, Komuro I. Roles of cardiac transcription factors in cardiac hypertrophy. *Circ Res.* 2003;92:1079–1088. doi: 10.1161/01.RES.0000072977.86706.23
7. Alexanian M, Padmanabhan A, McKinsey TA, Haldar SM. Epigenetic therapies in heart failure. *J Mol Cell Cardiol.* 2019;130:197–204. doi: 10.1016/j.yjmcc.2019.04.012
8. Padmanabhan A, Haldar SM. Drugging transcription in heart failure. *J Physiol.* 2020;598:3005–3014. doi: 10.1113/JP276745
9. Anand P, Brown JD, Lin CY, Qi J, Zhang R, Artero PC, Alaiti MA, Bullard J, Alazem K, Margulies KB, et al. BET bromodomains mediate transcriptional pause release in heart failure. *Cell.* 2013;154:569–582. doi: 10.1016/j.cell.2013.07.013
10. Spiltoir JI, Stratton MS, Cavasin MA, Demos-Davies K, Reid BG, Qi J, Bradner JE, McKinsey TA. BET acetyl-lysine binding proteins control pathological cardiac hypertrophy. *J Mol Cell Cardiol.* 2013;63:175–179. doi: 10.1016/j.yjmcc.2013.07.017
11. Dhalluin C, Carlson JE, Zeng L, He C, Aggarwal AK, Zhou MM. Structure and ligand of a histone acetyltransferase bromodomain. *Nature.* 1999;399:491–496. doi: 10.1038/20974
12. Taniguchi Y. The bromodomain and extra-terminal domain (BET) family: functional anatomy of BET paralogous proteins. *Int J Mol Sci.* 2016;17:1849.
13. Xu Y, Vakoc CR. Targeting cancer cells with BET bromodomain inhibitors. *Cold Spring Harb Perspect Med.* 2017;7:a026674.
14. Stathis A, Bertoni F. BET proteins as targets for anticancer treatment. *Cancer Discov.* 2018;8:24–36. doi: 10.1158/2159-8290.CD-17-0605
15. Lovén J, Hoke HA, Lin CY, Lau A, Orlando DA, Vakoc CR, Bradner JE, Lee TI, Young RA. Selective inhibition of tumor oncogenes by disruption of super-enhancers. *Cell.* 2013;153:320–334. doi: 10.1016/j.cell.2013.03.036
16. Nicodeme E, Jeffrey KL, Schaefer U, Beinke S, Dewell S, Chung CW, Chandwani R, Marazzi I, Wilson P, Coste H, et al. Suppression of inflammation by a synthetic histone mimic. *Nature.* 2010;468:1119–1123. doi: 10.1038/nature09589
17. Filippakopoulos P, Qi J, Picaud S, Shen Y, Smith WB, Fedorov O, Morse EM, Keates T, Hickman TT, Felletar I, et al. Selective inhibition of BET bromodomains. *Nature.* 2010;468:1067–1073. doi: 10.1038/nature09504
18. Duan Q, McMahon S, Anand P, Shah H, Thomas S, Salunga HT, Huang Y, Zhang R, Sahadevan A, Lemieux ME, et al. BET bromodomain inhibition suppresses innate inflammatory and profibrotic transcriptional networks in heart failure. *Sci Transl Med.* 2017;9:eaah5084.
19. Antolic A, Wakimoto H, Jiao Z, Gorham JM, DePalma SR, Lemieux ME, Conner DA, Lee DY, Qi J, Seidman JG, et al. BET bromodomain proteins regulate transcriptional reprogramming in genetic dilated cardiomyopathy. *JCI Insight.* 2020;5:e138687.
20. Houzelstein D, Bullock SL, Lynch DE, Grigorieva EF, Wilson VA, Beddington RS. Growth and early postimplantation defects in mice deficient for the bromodomain-containing protein Brd4. *Mol Cell Biol.* 2002;22:3794–3802. doi: 10.1128/mcb.22.11.3794-3802.2002
21. Love MI, Huber W, Anders S. Moderated estimation of fold change and dispersion for RNA-seq data with DESeq2. *Genome Biol.* 2014;15:550. doi: 10.1186/s13059-014-0550-8
22. Chen EY, Tan CM, Kou Y, Duan Q, Wang Z, Meirelles GV, Clark NR, Ma'ayan A. Enrichr: interactive and collaborative HTML5 gene list enrichment analysis tool. *BMC Bioinformatics.* 2013;14:128. doi: 10.1186/1471-2105-14-128
23. Sohal DS, Nghiem M, Crackower MA, Witt SA, Kimball TR, Tymitz KM, Penninger JM, Molkentin JD. Temporally regulated and tissue-specific gene manipulations in the adult and embryonic heart using a tamoxifen-inducible Cre protein. *Circ Res.* 2001;89:20–25. doi: 10.1161/hh1301.092687
24. Jiao K, Kulessa H, Tompkins K, Zhou Y, Batts L, Baldwin HS, Hogan BL. An essential role of Bmp4 in the atrioventricular septation of the mouse heart. *Genes Dev.* 2003;17:2362–2367. doi: 10.1101/gad.1124803
25. Lee JE, Park YK, Park S, Jang Y, Waring N, Dey A, Ozato K, Lai B, Peng W, Ge K. Brd4 binds to active enhancers to control cell identity gene induction in adipogenesis and myogenesis. *Nat Commun.* 2017;8:2217. doi: 10.1038/s41467-017-02403-5
26. Buenrostro JD, Giresi PG, Zaba LC, Chang HY, Greenleaf WJ. Transposition of native chromatin for fast and sensitive epigenomic profiling of open chromatin, DNA-binding proteins and nucleosome position. *Nat Methods.* 2013;10:1213–1218. doi: 10.1038/nmeth.2688
27. Heinz S, Benner C, Spann N, Bertolino E, Lin YC, Laslo P, Cheng JX, Murre C, Singh H, Glass CK. Simple combinations of lineage-determining transcription factors prime cis-regulatory elements required for macrophage and B cell identities. *Mol Cell.* 2010;38:576–589. doi: 10.1016/j.molcel.2010.05.004
28. Knowlton KU, Baracchini E, Ross RS, Harris AN, Henderson SA, Evans SM, Glembotski CC, Chien KR. Co-regulation of the atrial natriuretic factor and cardiac myosin light chain-2 genes during alpha-adrenergic stimulation of neonatal rat ventricular cells: identification of cis sequences within an embryonic and a constitutive contractile protein gene which mediate inducible expression. *J Biol Chem.* 1991;266:7759–7768.
29. Hsu A, Duan Q, McMahon S, Huang Y, Wood SA, Gray NS, Wang B, Bruneau BG, Haldar SM. Salt-inducible kinase 1 maintains HDAC7 stability

to promote pathologic cardiac remodeling. *J Clin Invest.* 2020;130:2966–2977. doi: 10.1172/JCI133753
30. Burridge PW, Matsa E, Shukla P, Lin ZC, Churko JM, Ebert AD, Lan F, Diecke S, Huber B, Mordwinkin NM, et al. Chemically defined generation of human cardiomyocytes. *Nat Methods.* 2014;11:855–860. doi: 10.1038/nmeth.2999
31. Koitabashi N, Bedja D, Zaiman AL, Pinto YM, Zhang M, Gabrielson KL, Takimoto E, Kass DA. Avoidance of transient cardiomyopathy in cardiomyocyte-targeted tamoxifen-induced MerCreMer gene deletion models. *Circ Res.* 2009;105:12–15. doi: 10.1161/CIRCRESAHA.109.198416
32. Arany Z, He H, Lin J, Hoyer K, Handschin C, Toka O, Ahmad F, Matsui T, Chin S, Wu PH, et al. Transcriptional coactivator PGC-1 alpha controls the energy state and contractile function of cardiac muscle. *Cell Metab.* 2005;1:259–271. doi: 10.1016/j.cmet.2005.03.002
33. Lehman JJ, Boudina S, Banke NH, Sambandam N, Han X, Young DM, Leone TC, Gross RW, Lewandowski ED, Abel ED, et al. The transcriptional coactivator PGC-1alpha is essential for maximal and efficient cardiac mitochondrial fatty acid oxidation and lipid homeostasis. *Am J Physiol Heart Circ Physiol.* 2008;295:H185–H196. doi: 10.1152/ajpheart.00081.2008
34. Alexanian M, Haldar SM. BETs that cover the spread from acquired to heritable heart failure. *J Clin Invest.* 2020;130:4536–4539. doi: 10.1172/JCI140304
35. Huang B, Yang XD, Zhou MM, Ozato K, Chen LF. Brd4 coactivates transcriptional activation of NF-kappaB via specific binding to acetylated RelA. *Mol Cell Biol.* 2009;29:1375–1387. doi: 10.1128/MCB.01365-08
36. Shi J, Wang Y, Zeng L, Wu Y, Deng J, Zhang Q, Lin Y, Li J, Kang T, Tao M, et al. Disrupting the interaction of BRD4 with diacetylated Twist suppresses tumorigenesis in basal-like breast cancer. *Cancer Cell.* 2014;25:210–225. doi: 10.1016/j.ccr.2014.01.028
37. Wu SY, Lee AY, Lai HT, Zhang H, Chiang CM. Phospho switch triggers Brd4 chromatin binding and activator recruitment for gene-specific targeting. *Mol Cell.* 2013;49:843–857. doi: 10.1016/j.molcel.2012.12.006
38. Asangani IA, Dommeti VL, Wang X, Malik R, Cieslik M, Yang R, Escara-Wilke J, Wilder-Romans K, Dhanireddy S, Engelke C, et al. Therapeutic targeting of BET bromodomain proteins in castration-resistant prostate cancer. *Nature.* 2014;510:278–282. doi: 10.1038/nature13229
39. Roe JS, Mercan F, Rivera K, Pappin DJ, Vakoc CR. BET bromodomain inhibition suppresses the function of hematopoietic transcription factors in acute myeloid leukemia. *Mol Cell.* 2015;58:1028–1039. doi: 10.1016/j.molcel.2015.04.011
40. He A, Gu F, Hu Y, Ma Q, Ye LY, Akiyama JA, Visel A, Pennacchio LA, Pu WT. Dynamic GATA4 enhancers shape the chromatin landscape central to heart development and disease. *Nat Commun.* 2014;5:4907. doi: 10.1038/ncomms5907
41. Akerberg BN, Gu F, VanDusen NJ, Zhang X, Dong R, Li K, Zhang B, Zhou B, Sethi I, Ma Q, et al. A reference map of murine cardiac transcription factor chromatin occupancy identifies dynamic and conserved enhancers. *Nat Commun.* 2019;10:4907. doi: 10.1038/s41467-019-12812-3
42. Durocher D, Chen CY, Ardati A, Schwartz RJ, Nemer M. The atrial natriuretic factor promoter is a downstream target for Nkx-2.5 in the myocardium. *Mol Cell Biol.* 1996;16:4648–4655. doi: 10.1128/mcb.16.9.4648
43. Grépin C, Dagnino L, Robitaille L, Haberstroh L, Antakly T, Nemer M. A hormone-encoding gene identifies a pathway for cardiac but not skeletal muscle gene transcription. *Mol Cell Biol.* 1994;14:3115–3129. doi: 10.1128/mcb.14.5.3115
44. Takaya T, Kawamura T, Morimoto T, Ono K, Kita T, Shimatsu A, Hasegawa K. Identification of p300-targeted acetylated residues in GATA4 during hypertrophic responses in cardiac myocytes. *J Biol Chem.* 2008;283:9828–9835. doi: 10.1074/jbc.M707391200
45. Lamonica JM, Deng W, Kadauke S, Campbell AE, Gamsjaeger R, Wang H, Cheng Y, Billin AN, Hardison RC, Mackay JP, et al. Bromodomain protein Brd3 associates with acetylated GATA1 to promote its chromatin occupancy at erythroid target genes. *Proc Natl Acad Sci U S A.* 2011;108:E159–E168. doi: 10.1073/pnas.1102140108
46. Gamsjaeger R, Webb SR, Lamonica JM, Billin A, Blobel GA, Mackay JP. Structural basis and specificity of acetylated transcription factor GATA1 recognition by BET family bromodomain protein Brd3. *Mol Cell Biol.* 2011;31:2632–2640. doi: 10.1128/MCB.05413-11
47. Wu SY, Chiang CM. The double bromodomain-containing chromatin adaptor Brd4 and transcriptional regulation. *J Biol Chem.* 2007;282:13141–13145. doi: 10.1074/jbc.R700001200
48. Filippakopoulos P, Picaud S, Mangos M, Keates T, Lambert JP, Barsyte-Lovejoy D, Felletar I, Volkmer R, Müller S, Pawson T, et al. Histone recognition and large-scale structural analysis of the human bromodomain family. *Cell.* 2012;149:214–231. doi: 10.1016/j.cell.2012.02.013
49. Jung M, Philpott M, Müller S, Schulze J, Badock V, Eberspächer U, Moosmayer D, Bader B, Schmees N, Fernández-Montalván A, et al. Affinity map of bromodomain protein 4 (BRD4) interactions with the histone H4 tail and the small molecule inhibitor JQ1. *J Biol Chem.* 2014;289:9304–9319. doi: 10.1074/jbc.M113.523019
50. Romero FA, Taylor AM, Crawford TD, Tsui V, Côté A, Magnuson S. Disrupting acetyl-lysine recognition: progress in the development of bromodomain inhibitors. *J Med Chem.* 2016;59:1271–1298. doi: 10.1021/acs.jmedchem.5b01514
51. Dawson MA. The cancer epigenome: concepts, challenges, and therapeutic opportunities. *Science.* 2017;355:1147–1152. doi: 10.1126/science.aam7304
52. Piha-Paul SA, Sachdev JC, Barve M, LoRusso P, Szmulewitz R, Patel SP, Lara PN Jr, Chen X, Hu B, Freise KJ, et al. First-in-human study of mivebresib (ABBV-075), an oral pan-inhibitor of bromodomain and extra terminal proteins, in patients with relapsed/refractory solid tumors. *Clin Cancer Res.* 2019;25:6309–6319. doi: 10.1158/1078-0432.CCR-19-0578
53. Ray KK, Nicholls SJ, Buhr KA, Ginsberg HN, Johansson JO, Kalantar-Zadeh K, Kulikowski E, Toth PP, Wong N, Sweeney M, et al; BETonMACE Investigators and Committees. Effect of apabetalone added to standard therapy on major adverse cardiovascular events in patients with recent acute coronary syndrome and type 2 diabetes: a randomized clinical trial. *JAMA.* 2020;323:1565–1573. doi: 10.1001/jama.2020.3308
54. Winter GE, Buckley DL, Paulk J, Roberts JM, Souza A, Dhe-Paganon S, Bradner JE. Drug development: phthalimide conjugation as a strategy for in vivo target protein degradation. *Science.* 2015;348:1376–1381. doi: 10.1126/science.aab1433
55. Lu J, Qian Y, Altieri M, Dong H, Wang J, Raina K, Hines J, Winkler JD, Crew AP, Coleman K, et al. Hijacking the E3 ubiquitin ligase cereblon to efficiently target BRD4. *Chem Biol.* 2015;22:755–763. doi: 10.1016/j.chembiol.2015.05.009
56. Zhou B, Hu J, Xu F, Chen Z, Bai L, Fernandez-Salas E, Lin M, Liu L, Yang CY, Zhao Y, et al. Discovery of a small-molecule degrader of bromodomain and extra-terminal (BET) proteins with picomolar cellular potencies and capable of achieving tumor regression. *J Med Chem.* 2018;61:462–481. doi: 10.1021/acs.jmedchem.6b01816
57. Stratton MS, Bagchi RA, Felisbino MB, Hirsch RA, Smith HE, Riching AS, Enyart BY, Koch KA, Cavasin MA, Alexanian M, et al. Dynamic chromatin targeting of BRD4 stimulates cardiac fibroblast activation. *Circ Res.* 2019;125:662–677. doi: 10.1161/CIRCRESAHA.119.315125
58. Garg V, Kathiriya IS, Barnes R, Schluterman MK, King IN, Butler CA, Rothrock CR, Eapen RS, Hirayama-Yamada K, Joo K, et al. GATA4 mutations cause human congenital heart defects and reveal an interaction with TBX5. *Nature.* 2003;424:443–447. doi: 10.1038/nature01827
59. Molkentin JD, Lin Q, Duncan SA, Olson EN. Requirement of the transcription factor GATA4 for heart tube formation and ventral morphogenesis. *Genes Dev.* 1997;11:1061–1072. doi: 10.1101/gad.11.8.1061
60. Ieda M, Fu JD, Delgado-Olguin P, Vedantham V, Hayashi Y, Bruneau BG, Srivastava D. Direct reprogramming of fibroblasts into functional cardiomyocytes by defined factors. *Cell.* 2010;142:375–386. doi: 10.1016/j.cell.2010.07.002
61. Fu JD, Stone NR, Liu L, Spencer CI, Qian L, Hayashi Y, Delgado-Olguin P, Ding S, Bruneau BG, Srivastava D. Direct reprogramming of human fibroblasts toward a cardiomyocyte-like state. *Stem Cell Reports.* 2013;1:235–247. doi: 10.1016/j.stemcr.2013.07.005
62. Qian L, Huang Y, Spencer CI, Foley A, Vedantham V, Liu L, Conway SJ, Fu JD, Srivastava D. In vivo reprogramming of murine cardiac fibroblasts into induced cardiomyocytes. *Nature.* 2012;485:593–598. doi: 10.1038/nature11044
63. Stone NR, Gifford CA, Thomas R, Pratt KJB, Samse-Knapp K, Mohamed TMA, Radzinsky EM, Schricker A, Ye L, Yu P, et al. Context-specific transcription factor functions regulate epigenomic and transcriptional dynamics during cardiac reprogramming. *Cell Stem Cell.* 2019;25:87–102.e9. doi: 10.1016/j.stem.2019.06.012
64. Hashimoto H, Wang Z, Garry GA, Malladi VS, Botten GA, Ye W, Zhou H, Osterwalder M, Dickel DE, Visel A, et al. Cardiac reprogramming factors synergistically activate genome-wide cardiogenic stage-specific enhancers. *Cell Stem Cell.* 2019;25:69–86.e5. doi: 10.1016/j.stem.2019.03.022
65. Oka T, Maillet M, Watt AJ, Schwartz RJ, Aronow BJ, Duncan SA, Molkentin JD. Cardiac-specific deletion of Gata4 reveals its requirement for hypertrophy, compensation, and myocyte viability. *Circ Res.* 2006;98:837–845. doi: 10.1161/01.RES.0000215985.18538.c4

66. Heineke J, Auger-Messier M, Xu J, Oka T, Sargent MA, York A, Klevitsky R, Vaikunth S, Duncan SA, Aronow BJ, et al. Cardiomyocyte GATA4 functions as a stress-responsive regulator of angiogenesis in the murine heart. *J Clin Invest.* 2007;117:3198–3210. doi: 10.1172/JCI32573
67. Neubauer S. The failing heart: an engine out of fuel. *N Engl J Med.* 2007;356:1140–1151. doi: 10.1056/NEJMra063052
68. Huss JM, Kelly DP. Mitochondrial energy metabolism in heart failure: a question of balance. *J Clin Invest.* 2005;115:547–555. doi: 10.1172/JCI24405
69. Bates MG, Bourke JP, Giordano C, d'Amati G, Turnbull DM, Taylor RW. Cardiac involvement in mitochondrial DNA disease: clinical spectrum, diagnosis, and management. *Eur Heart J.* 2012;33:3023–3033. doi: 10.1093/eurheartj/ehs275
70. El-Hattab AW, Scaglia F. Mitochondrial cardiomyopathies. *Front Cardiovasc Med.* 2016;3:25. doi: 10.3389/fcvm.2016.00025
71. Dufour CR, Wilson BJ, Huss JM, Kelly DP, Alaynick WA, Downes M, Evans RM, Blanchette M, Giguère V. Genome-wide orchestration of cardiac functions by the orphan nuclear receptors ERRalpha and gamma. *Cell Metab.* 2007;5:345–356. doi: 10.1016/j.cmet.2007.03.007
72. Stefanovic S, Christoffels VM. GATA-dependent transcriptional and epigenetic control of cardiac lineage specification and differentiation. *Cell Mol Life Sci.* 2015;72:3871–3881. doi: 10.1007/s00018-015-1974-3
73. Shi J, Vakoc CR. The mechanisms behind the therapeutic activity of BET bromodomain inhibition. *Mol Cell.* 2014;54:728–736. doi: 10.1016/j.molcel.2014.05.016
74. Faivre EJ, McDaniel KF, Albert DH, Mantena SR, Plotnik JP, Wilcox D, Zhang L, Bui MH, Sheppard GS, Wang L, et al. Selective inhibition of the BD2 bromodomain of BET proteins in prostate cancer. *Nature.* 2020;578:306–310. doi: 10.1038/s41586-020-1930-8
75. Gilan O, Rioja I, Knezevic K, Bell MJ, Yeung MM, Harker NR, Lam EYN, Chung CW, Bamborough P, Petretich M, et al. Selective targeting of BD1 and BD2 of the BET proteins in cancer and immunoinflammation. *Science.* 2020;368:387–394. doi: 10.1126/science.aaz8455
76. Jang MK, Mochizuki K, Zhou M, Jeong HS, Brady JN, Ozato K. The bromodomain protein Brd4 is a positive regulatory component of P-TEFb and stimulates RNA polymerase II-dependent transcription. *Mol Cell.* 2005;19:523–534. doi: 10.1016/j.molcel.2005.06.027
77. Yang Z, Yik JH, Chen R, He N, Jang MK, Ozato K, Zhou Q. Recruitment of P-TEFb for stimulation of transcriptional elongation by the bromodomain protein Brd4. *Mol Cell.* 2005;19:535–545. doi: 10.1016/j.molcel.2005.06.029
78. Shen C, Ipsaro JJ, Shi J, Milazzo JP, Wang E, Roe JS, Suzuki Y, Pappin DJ, Joshua-Tor L, Vakoc CR. NSD3-short is an adaptor protein that couples BRD4 to the CHD8 chromatin remodeler. *Mol Cell.* 2015;60:847–859. doi: 10.1016/j.molcel.2015.10.033
79. Rahman S, Sowa ME, Ottinger M, Smith JA, Shi Y, Harper JW, Howley PM. The Brd4 extraterminal domain confers transcription activation independent of pTEFb by recruiting multiple proteins, including NSD3. *Mol Cell Biol.* 2011;31:2641–2652. doi: 10.1128/MCB.01341-10
80. Lambert JP, Picaud S, Fujisawa T, Hou H, Savitsky P, Uusküla-Reimand L, Gupta GD, Abdouni H, Lin ZY, Tucholska M, et al. Interactome rewiring following pharmacological targeting of BET bromodomains. *Mol Cell.* 2019;73:621–638.e17. doi: 10.1016/j.molcel.2018.11.006